

*Evolution of high dielectric constant Perovskite- Calcium Copper Titanate by Modified Solid State Process and its Characterization*

*A thesis submitted in partial fulfillment of the requirement for the award of the degree of*

**Master of Technology**  
In  
**Material Engineering**

*Submitted by*

**ASHNARAYAN SAH**

**Exam Roll No.:** M4MAT19002  
**Class Roll No.:**001711303022  
**Registration No.**140912 of 17-18

*Under the guidance of*

**Dr. Sathi Banerjee**  
(Assistant Professor)

Department of Metallurgical and Material Engineering  
Jadavpur University, Kolkata-700032

**Dr.SoumyaMukherjee**

(Assistant Professor)

*Department of Metallurgy, School of Mines & Metallurgy*

*Kazi Nazrul University, Asansol-713340*

**JADAVPUR UNIVERSITY**  
**Kolkata-700032**

**CERTIFICATE**

*This is to certify that the thesis entitled “**Calcium Copper titanate by modified Solid State Process and its characterization**” been carried out under the combine guidance of Dr. SathiBanerjee, Dept. of Metallurgical and Material Engineering, Jadavpur University and Dr. Soumya Mukherjee co-superviosor, Department of Metallurgy,kazi Nazrul, Asansol by Ashnarayan sah during the academic session 2018-2019 in partial fulfillment of the requirement for the award of the degree of Master of Technology in Material Engineering in the Department of Metallurgical and Material Engineering, Jadavpur University, Kolkata- 700032. In our opinion the work fulfils the requirement for which it is submitted. It is further certified that materials obtained from other sources have been acknowledged in the thesis.*

-----  
**-Dr. Sathi Banerjee**  
Department of Metallurgical  
and Material Engineering  
Jadavpur University  
Kolkata-700032

-----  
**Dr. Soumya Mukherjee**  
Department of Metallurgical,  
Kazi Nazurul University  
Asansol-713340

-----  
**Dr. Akashy Kumar Pramanick**  
**(Head of the Department)**  
Department of Metallurgical  
and Material Engineering

-----  
**Dean, Faculty of Engineering  
and Technology**  
Jadavpur University  
Kolkata-700032

## *CERTIFICATE OF EXAMINATION*

The forgoing thesis is hereby approved as credible study of engineering subject carried out and represented in a manner of warrants its acceptance as a prerequisite to the degree for which it has been submitted. It is to be understood that by the approval of the undersigned does not necessarily endorse any statement made, opinion, opinion expressed or conclusion drawn there in but approved the thesis only for the purpose for which it has been submitted.

### **Final Examiners for Evaluation of thesis**

1)

2)

3)

*Date:*

*Signature of Examiners*

## ACKNOWLEDGEMENT

I am deeply grateful to my department for giving me the opportunity to take up this interesting project work. It is my privilege to convey my heartiest thanks to my thesis supervisor **Dr. Sathi Banerjee**, Department of Metallurgical and Material Engineering, Jadavpur University, Kolkata-700032. I owe to her for her sincere help and constructive guidance rendered to me during thesis work. I am especially thankful to **Dr. Soumya Mukherjee Co-Spervisor**, Department of Metallurgy, School of Mines and Metallurgy, Kazi Nazrul University, Asansol. His close guidance helped me to do my work more efficiently.

I would like to sincerely express my earnest gratitude to **Prof. Akshay Kumar Pramanick (HOD)** for his permission to use different characterizations and lab facilities during project work. I also express my sincere thanks to **Dr. Kalyan Kumar Chattopadhyay**, Director, School of Materials Science and Nanotechnology, Jadavpur University for his help to stand this project. I would like to convey my heartiest thanks to all the faculty and staff members for their valuable guidance and support during the implementation of the project. I am thankful to **Mr. Sudhir Ghosh**, and **Mr. Jayanta Bhattacharya** for their constant support in laboratory testing. I thank to **MD. Shahnawaz, Srinath Ranjan Ghosh, Chirantan Mukherjee**, and **Pritha Pal**, research Scholars of Jadavpur University. Finally, I would like to thank all of my friends for their close assistance, encouragement and love throughout my project work. The guidance and help received from all the members who contributed to this project work was vital for the success of this project. I am grateful to all of you.

DATE:

ASHNARAYAN SAH

***Dedicated to my***

***PARENTS***

***for their support and encouragement.....***

## ***Table of content***

### ***ABSTRACT***

	<b>Page No.</b>
<b>CHAPTER 1: Introduction</b>	
1. Insulators	1
2. Dielectrics	2
3. Polarization in dielectric	3
4. Calcium copper titanate (CCTO)	4
5. Importance of CCTO system	5
6. Colossal Dielectric constant in CCTO	6
7. Origin of electrical properties	7
8. Dielectric properties of CCTO	8
<b>CHAPTER-2 Literature survey</b>	<b>9</b>
1. Different modes of synthesis of CCTO	10
2. Discussion	13
3. Objective	14
<b>CHAPTER-3 Characterization techniques</b>	<b>15</b>
1. X-ray diffraction (XRD)	16
2. XRD analysis	17
3. Feature & basic principal of XRD	19

4. Scanning electron microscope	20
5. FESEM	23
6. FTIR	25
7. Dielectric measurement	26
<b>CHAPTER-4 EXPERIMENTAL WORK</b>	<b>27</b>
1. Preamble	28
2. Experimental procedure	30
<b>CHAPTER-5 Result &amp; Discussion</b>	<b>32</b>
1. XRD Analysis	38
2. FE SEM Analysis	40
3. FTIR Analysis	42
4. Dielectric Measurements	45
<b>CHAPTER-6 CONCLUSIONS&amp; FUTURE SCOPE</b>	<b>46</b>
<b>Reference</b>	<b>52</b>
<b>Appendix</b>	<b>56</b>

## ***ABSTRACT***

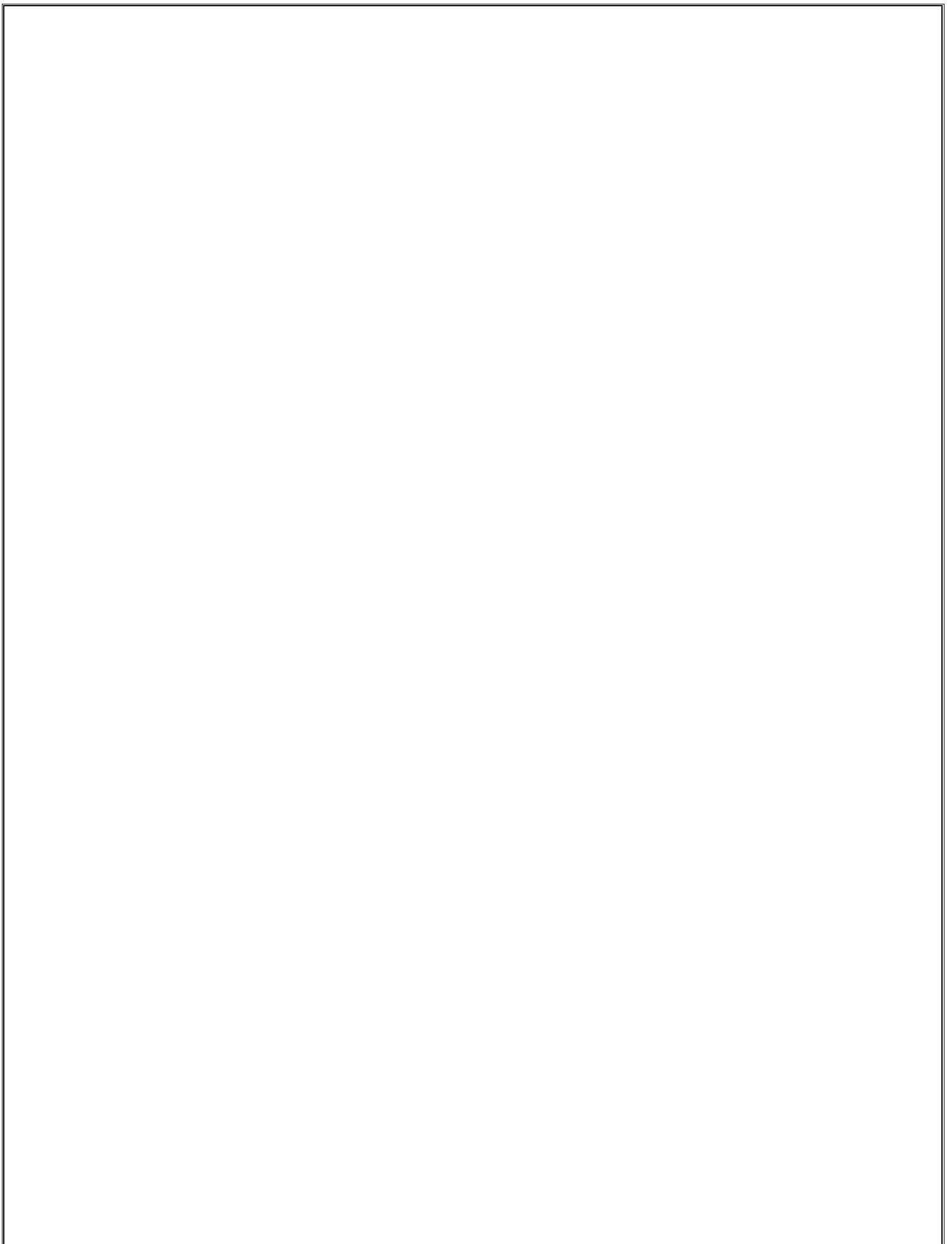
Perovskite calcium copper titanate possesses a giant dielectric constant making it a suitable candidate for possible applications in microelectronic components, advanced transistors, energy storage capacitors. Generally, this grade of material is synthesized by a chemical route to improve homogeneity, controlled size growth for enhanced properties. Moreover, dielectric constant of this compound is found to be stable at higher temperature within 100-600K in contrast to PZT, Barium titanate where it deteriorates with temperature due to lower Curie temperature. In the present research, a simple synthesis process is adopted using precursors of high purity oxides like Calcium carbonate, Titania, Copper oxide without any costly chemical precursors and complicated synthesis routes. Molar ratio of oxides used is about 1:3:4 with mechano-chemical activation in an agate mortar for 20, 25 and 30 hours respectively in dry condition. After milling, powders obtained are made to undergo annealing at a fixed temperature of 900°C for 26 hours soaking period. Phase analysis was carried to determine the phase along with crystallite size calculation. Bond formation of the synthesized doped sample was analyzed to obtain the M-O coordination and vibration-stretching analysis of the bonds. Morphological features are also noted using FESEM for topographical features. Both FTIR and XRD analyses confirm the compound formation in terms of molecular structure responsible to obtain the proper phase. Dielectric measurement is done in frequency range 1 kHz to 1MHz. The electric properties such as dielectric loss and dielectric constant were studied as a function of frequency and temperature, which show a diffused phase transition.

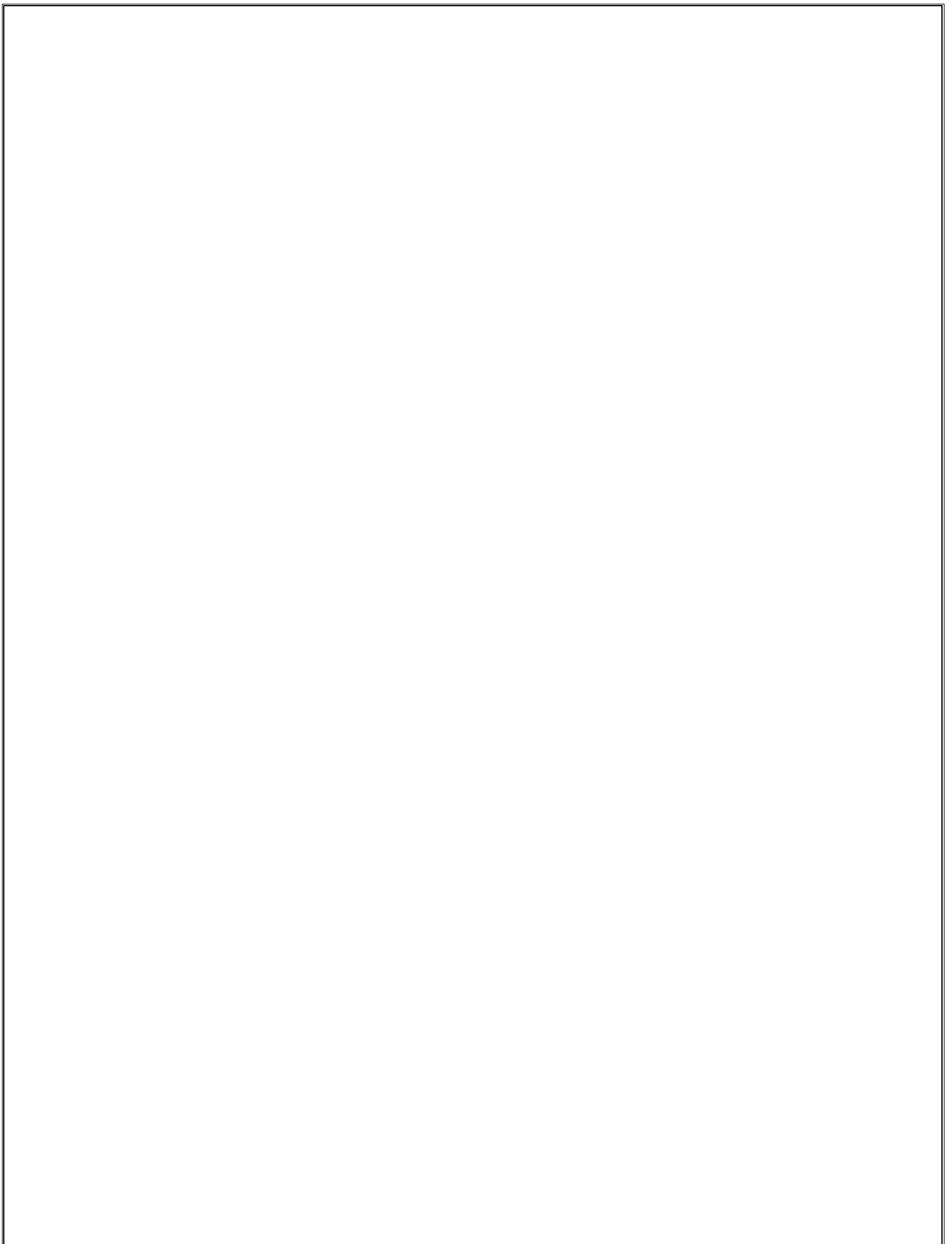


# **CHAPTER – 1**



## **INTRODUCTION**





# Introduction

## 1 Insulator

An electrical insulator is a material whose internal electric charges do not flow freely, but under the influence of an electric field. Very little electric current will flow through it. This contrasts with other materials, semiconductors and conductors, which conduct electric current, more easily. An insulator which is perfect does not exist in nature, but some materials such as, paper, glass, mica and polythene etc having higher resistivity are very good electrical insulators. Larger classes of materials not having higher bulk resistivity are also good enough to insulate electrical wirings and cables. Some of the examples are rubber-like polymers and most plastics. Almost all insulators have large band gap about 6eV as compared to semiconductor and conductor. This is because of the "valence" band consisting of the highest energy electrons is full, and the next band is separated from it by a large energy gap above it. There is always some voltage named as breakdown voltage that will give the electrons enough energy to be excited into this band. Once the breakdown voltage is exceeded the material discontinues being an insulator, and charge starts passing through it. Insulators are commonly used as a flexible coating on electric wire and cable which prevents a dangerous electrical shock when we touch the wire. These are the common classes of insulators: pin type insulators, Post insulator, Suspension insulator, strain insulators and Shackle insulator and Bushing insulators etc.[1]

## **2. Dielectrics**

A dielectric constant of this compound is found to be stable at higher temperature within 100-600K [2, 3] in contrast to PZT, Barium titanate where it deteriorates with temperature due to lower Curie temperature. A dielectric is an electrical insulator that can be polarized only when applying an applied electric field [4]. Whenever a dielectric is placed in an electric field, electric charges stop flowing through the material but slightly shift from their average equilibrium positions causing dielectric polarization. Due to dielectric polarization, positive charges are displaced in the direction of the electric field while negatively charged are displaced in the opposite direction of the electric field. The term dielectric is used to indicate the energy storing capacity of the material. The study of dielectric properties concerns storage and dissipation of electric and magnetic energy in material [5]. An example of a dielectric is placing a ceramic material between the metallic plates of a capacitor. If the voltage across a dielectric material becomes too great or if the electrostatic field becomes too strong the material will suddenly begin to conduct current. This process is called dielectric breakdown. An important property of a dielectric is its ability to support an electrostatic field while dissipating minimum energy in the form of heat. The lower the dielectric loss of a material the more effective is that dielectric material. Another thing which comes into consideration is the dielectric constant which describes the extent to which a substance concentrates the electrostatic lines of flux. Some of the substances having a low dielectric constant are perfect vacuum, dry air, and most pure and dry gases such as helium and nitrogen. Materials having moderate dielectric constants include ceramics, distilled water; glass etc Metal oxides mostly have high dielectric constants.

## **3. Polarization of dielectric**

Dielectric polarization occurs when a dipole moment is formed in an insulating material because of an externally applied electric field. When a current interacts with a dielectric (insulating) material, the dielectric material will respond with a shift in charge distribution with the positive charges aligning with the electric field and the negative charges aligning against it. By taking advantage of this response, important circuit elements such as capacitors can be made.

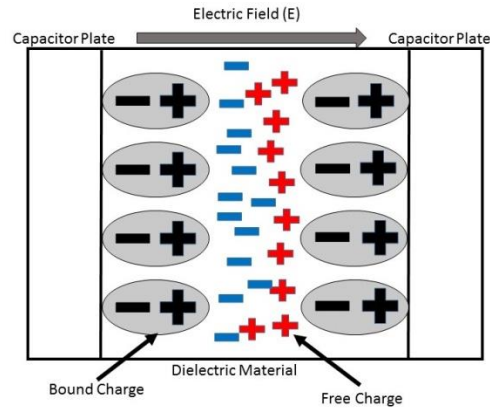


**Figure 3.1 Polarisation of Dielectric**

### Dielectrics are subdivided into two groups

- 1) Non-Polar dielectrics which behave as an insulator
- 2) Polar dielectrics are the dielectrics in which the molecules or atoms possess a permanent dipole moment which is ordinarily randomly oriented and becomes more or less oriented by the application of an external electric field. If a material contains polar materials, they will be in random orientations but without any electric field. On applying electric field it will be polarized. This will cause increase in the capacitance of the parallel plate structure. The presence of any dielectric material decreases the electric field produced by a given charge density [6].

$$E_{\text{effective}} = E - E_{\text{polarization}} = \frac{\sigma}{k\epsilon_0}$$

Here  $k$  = dielectric constant of the material

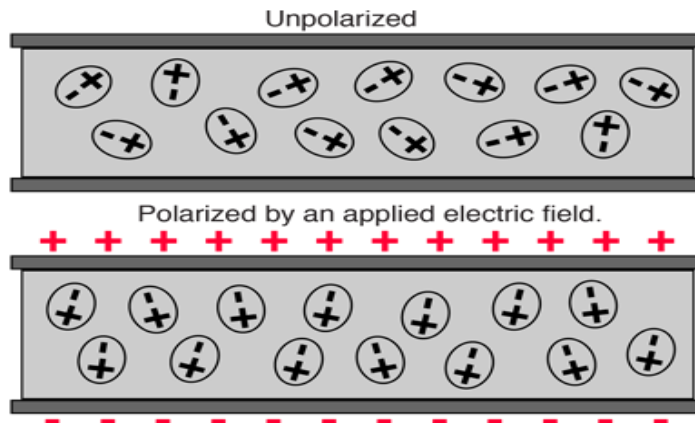


Figure 3.2 Polarisation of Dielectric

#### 4. Calcium copper titanate (CCTO)

Calcium copper titanate is an inorganic compound with the formula  $\text{CaCu}_3\text{Ti}_4\text{O}_{12}$ . It is noteworthy for its extremely large dielectric constant (effective relative permittivity) of in excess of 10,000 at room temperature [7]. Calcium copper titanate,  $\text{CaCu}_3\text{Ti}_4\text{O}_{12}$  (CCTO) is a perovskite structure that has a body-centered cubic crystal structure with slightly tilted  $[\text{TiO}_6]$  octahedra facing each other [8, 9]. CCTO ceramics exhibit ferroelectric (FE) hysteresis loops, despite the fact that it belongs to the centro symmetric space group. Remnant polarization and coercive field values were found to be strongly dependent on the sintering conditions. This material shows huge dielectric constant ( $\epsilon_r$ ) sometimes larger than  $50 \times 10^3$ , over a wide temperature range, i.e. from 100 to 400K [10]. Due to high  $\epsilon_r$ , elaborative investigations were done on this topic such as the influence of the microstructure, electrode material and pellet thickness on impedance and dielectric characteristics. CCTO is also utilized to manufacture many of the electronic components such as multilayer capacitor, electronic devices in automobiles and aircrafts. They can also be applied to important devices such as DRAM (Dynamic Random Access Memory), microwave device and many more. Since CCTO structure is derived from the cubic perovskite by an octahedral tilt distortion, this is caused due to the size mismatch and the nature of the A cations. The  $\text{TiO}_6$  octahedral tilt to produce a structure where three quarters of the A sites have square-planar coordination and are occupied by Jahn-Teller  $\text{Cu}^{2+}$  ions. The remaining quarters of the sites is occupied by Calcium [11].

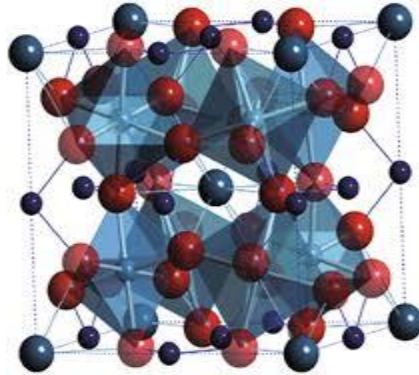


Fig4.1 The structure of  $\text{CaCu}_3\text{Ti}_4\text{O}_{12}$  shown as  $\text{TiO}_6$  octahedra, Cu in square planar coordination O ions at the centre of each face and edge and Ca at the origin and Cu centre (red spheres)[12].

## 5. Importance of CCTO system

The dielectric properties of CCTO makes a desirable material for micro-electric applications such as static and dynamic random access memories, high dielectric capacitors, and thin film devices. Ordinarily, dielectric constants higher than 1000 are related to ferroelectric or relaxor properties. The interesting feature observed in CCTO ceramics is the existence of a nonlinear current–voltage characteristic [13, 14]. This non-Ohmic behaviour was considered to be due to Schottky-type electrostatic barriers at the grain boundaries [13, 15]. These results seem to support the idea of an extrinsic origin for the ultrahigh dielectric properties [16]. All these large dielectric constant materials have similar dielectric behaviour, i.e., they all exhibit a Debye-like relaxation and their dielectric constants are nearly independent of frequency and temperature well below the relaxation frequency. Usually large dielectric constants are found in ferroelectric materials. CCTO is non-ferroelectric and has no structural changes down to 35 K. The dielectric properties make CCTO a desirable material for micro-electric applications such as static and dynamic random access memories and thin film devices. This material exhibits no crystallographic structural phase transition, associated with spontaneous polarization. The ultra-miniaturization of electronic devices in automobiles and aircraft requires the development of high dielectric materials that should be stable over a wide range of temperatures. Research indicates that  $\text{CaCu}_3\text{Ti}_4\text{O}_{12}$  may be part of a new class of oxide perovskite whose high dielectric properties are different than classic ferroelectrics or relaxors. Diffraction experiments detect no



presence of superstructure peaks or diffuse scattering or broadening in Bragg intensities which are often indicative of nano domains or disorder effects that are associated with relaxors.

## 6. Colossal dielectric constant in CCTO

The colossal dielectric constant (CDC) phenomenon, which was firstly observed in  $\text{CaCu}_3\text{Ti}_4\text{O}_{12}$  (CCTO) ceramics through intensive investigations which were conducted in both experimental and theoretical ways at bulk ceramics, single crystals [17,18] and polycrystalline as well as epitaxial thin films on various substrates [19,20]. All of these samples showed the characteristic CDC features. In the year 2002, D.Sinclair et al. concluded from impedance spectroscopy that CCTO ceramics is electrically heterogeneous which composed of semiconducting grains having insulating grain boundaries, and attributes the CDC phenomenon an internal barrier layer capacitance (IBLC) [21]. This explanation proved to be correct for the ceramic CCTO case, but formed difficulties when it was applied to the single crystals, nevertheless show the CDC phenomenon [22]. The IBLC model is supported by the fact that CCTO grains are semiconducting [23, 24]. However, the contradictive fact is that the CCTO optical band gap of 2.5eV predicted a good dielectric material below the room temperature.  $I$ - $V$  and  $C$ - $V$  measurements indicated that Schottky barriers or metal insulator- semiconductor (MIS) junctions were formed at the thin film top electrode interfaces [25]. By annealing at an intermediate temperature in air, the CDC state can be converted to a non-CDC state, where we able to observe the intrinsic dielectric properties of the sample. The XPS profiles of the CDC and non-CDC states showed that they corresponded to low and high Cu oxidization states respectively [26]. In order to account for the semi-conductivity in CCTO, two models have been proposed so far. First, it is known that  $\text{TiO}_2$ -based perovskite ceramics such as  $\text{BaTiO}_3$  and  $\text{SrTiO}_3$  become more conductive during sintering under reducing conditions due to a small amount of oxygen loss occurring at high temperatures. On the other hand, a cationic non-stoichiometric model was suggested. With the recent report that a  $\text{Cu}_2\text{O}$  phase was observed inside a decomposition zone with a negligible change in bulk resistivity during nitrogen or oxygen annealing, the semiconducting behaviour in CCTO is due to no stoichiometric model.

## **7. Origin of electrical properties**

The origin of giant static dielectric constant is not fully understood, though explanations in terms of atomic structure, microstructure, and extrinsic interface structure have been proposed. Based on the micro-structural evidence including domain boundaries in polycrystalline CCTO and twin boundaries in single crystal CCTO, it has been generally understood that a purely intrinsic model cannot be used to explain the origin of the high dielectric constant. Rather, it has been proposed that the reason for the abnormally large dielectric constant is due to Maxwell–Wagner relaxation, which was supported by a first-principles study. Here, the electrical heterogeneity originating from the mobile charged species and the internal interfaces in polycrystalline CCTO gives rise to the polarization in semiconducting grains and insulating grain boundaries. The grain boundary inhomogeneity was confirmed by the existence of electrical potential barriers via current–voltage measurements. So far, the internal barrier layer capacitor (IBLC) model has been widely accepted as the most likely mechanism to make clear the high dielectric constant in CCTO [27].

## **8. Dielectric properties of CCTO**

We found that the perovskite-related body-centered cubic materials  $\text{CaCu}_3\text{Ti}_4\text{O}_{12}$  (CCTO) exhibited in giant dielectric constant at room temperature and also the dielectric constant between 100 and 400 K of this compound is found to be stable at higher temperature within 100–600K in contrast to PZT, Barium titanate where it deteriorates with temperature due to lower curie temperature. These properties are very important for device implementation and microelectronic application but its nature and characteristics remain unsolved. From the structural studies we found that CCTO maintains a cubic structure without phase transitions. [28].

## **CHAPTER-2**

---

### **LITERATURE REVIEW**

## LITERATURE REVIEW

### Different Modes of Synthesis of CCTO

1. Solid state synthesis
2. Sol-gel method
3. Pulsed layer deposition
4. Chemical layer deposition
5. Wet-chemistry method
6. Combustion synthesis technique
7. Co-precipitation method
8. Precursor oxalate route
9. Chemical layer deposition

**1) X.H Zheng et al. [29]** The CCTO ceramics were prepared using conventional solid-state reaction method. Using starting materials of  $\text{CaCO}_3$  (>99%),  $\text{CuO}$   $\text{TiO}_2$ (>99%). Stoichiometric amounts of powders were mixed with distilled water by ball milling with zirconia media for 12 hr. After that the mixed powder were calcined in air at  $950^\circ\text{C}$  for 2hr. The calcined powder were again milled, by mixing 5wt percentages PVA as binder and pressed into disk of 13mm in diameter and 1-2 mm in thickness. These disk was sintered at temperature range  $1000^\circ\text{C}$  to  $1150^\circ\text{C}$  with different time and cooled to room temperature in furnace. This sample was characterized by XRD, FESEM, FTIR, FESEM and dielectric measurement. The crystalline phase was identified by X-ray diffraction analysis with  $\text{Cu K}\alpha$  radiation (XRD, D/max-IIIC). Microstructure of the ceramics was carried out in a field effect scanning electron microscope. The dielectric measurement and impedance analysis of the present CCTO ceramics were determined using precise LCR meter in the frequency range 20 Hz to 1MHz with temperature range  $25$ - $120^\circ\text{C}$ .  $\text{CaCu}_3\text{Ti}_4\text{O}_{12}$  (CCTO) ceramics were sintered with different temperature. The strong sintering effect on microstructure was found in  $\text{CaCu}_3\text{Ti}_4\text{O}_{12}$  (CCTO) ceramics. The approximate extended sintering time would benefit for formation of bigger and uniform grains of CCTO ceramics. Here the samples sintered at  $1120^\circ\text{C}$  for 6 hr gave the highest value of

permittivity about 12,400. Further the large result in higher permittivity. According to the impedance spectroscopy of CCTO grain size ceramic, related high permittivity could be associated Maxwell-Wagner model, which results from semiconducting grain and insulating grain boundary.

**2 )Julie J. Mohamed *et al.* [30]** The  $\text{CaCu}_3\text{Ti}_4\text{O}_{12}$  (CCTO) synthesized by the solid state reaction route. The sample were calcined at 900oC for 12 hrs and sintered at 1050°C for 24 hrs. The increase in sintering temperature found to improve the density and secondary phase formation of  $\text{Cu}_2\text{O}$ . A clear grain boundary and a dense microstructure were seen in the sintered samples. We absorbed that the sample sintered at 1040°C for 10 hrs yielded a uniform grain size with the highest permittivity.

**3) B.A.Bender *et al.* [31]** The  $\text{CaCu}_3\text{Ti}_4\text{O}_{12}$  (CCTO) ceramics prepared by using conventional solid state reaction for 3 h. Then XRD was used phase evolution for the various mixed powders and resultant discussion. Microstructure to monitor characterization was done on the fracture surfaces using scanning electron microscopy (SEM). The capacitance and dielectric loss of each sample were measured as a function of frequency (100 Hz to 100 kHz) and temperature (-50 to 100°C) and then use an integrated, computer controlled system. The dielectric properties of a standard processed sample (AM2) were also measured as a function of dc processing techniques. The standard sintering conditions was considered to be 1100°C for bias using a high voltage power supply in combination with a blocking circuit to protect the LCR meter (Hewlett-Packard 4284A) from the dc bias voltage.

**4) B. Barbier [32]** Dielectric properties of  $\text{CaCu}_3\text{Ti}_4\text{O}_{12}$  (CCTO)-based ceramics and thick films ( $e \sim 50\mu\text{m}$ ) prepared from powders synthesized by a chemical route method (co-precipitation) are presented and discussed. The characteristics of pellets and thick films are compared. The pellets exhibit high values of the dielectric permittivity ( $\epsilon_r \sim 1.4 \times 10^5$ ) and relatively small dielectric losses ( $\tan \delta \sim 0.16$ ) at 1 kHz and room temperature. These properties are independent of the nature of the metallization of the electrodes. In addition, the dielectric permittivity decreases when the diameter of the electrodes of the pellets increases, while the losses remain constant. This result, which is strongly related to the nature of the dielectric material in between the electrodes, constitutes a strong indication that the high dielectric permittivity values observed in this material are not related to an interfacial (electrode material) related mechanism but is an

internal barrier layer capacitor (IBLC) type. Very high values of the dielectric permittivity of CCTO thick films are measured ( $\epsilon_r \sim 5 \times 10^4$ ). The differences in dielectric permittivity between thick films and dense pellets may be attributed to the difference in grain size due to different CuO contents, and to the different reactivity of the materials.

**5) Zhu et al. [33]** The Prepared CCTO by oxalate co- precipitation method which is done at lower temperature with shorter reaction time as compared to the conventional solid state reaction. The precipitation containing stoichiometric amounts of the metal cations were heat treated to achieve single phase CCTO. DTA/TGA was carried out on a dried precipitate to study the thermal decomposition process. The phase's microstructure and dielectric properties of the sample were characterized by X ray diffraction, scanning electron microscopy and precision impedance analyzer.

**6) Thomas et al. [34]** Synthesized nanoparticles of CCTO from a precursor route. A method of preparing the nano particles of CCTO with the crystallite size varying from 30 to 200nm is optimized at a temperature as low as 680°C from the exothermic thermal decomposition of an precursor  $\text{CaCu}_3(\text{TiO})_4(\text{C}_2\text{O}_4)_8 \cdot 9\text{H}_2\text{O}$ . The phase singularity of the complex oxalate precursor is confirmed by the wet chemical analyses, X- ray diffraction, FT-IR and TGA/DTA analyses. The UV is reflectance and ESR spectra of CCTO powders indicate that the Cu (II) coordination changes from distorted octahedral to nearly flatten tetrahedral to square planar geometry with increasing annealing temperature. The HRTEM images have revealed that the evolution of the microstructure in nano scale is related to the change in Cu (II) coordination around the surface regions for the chemically prepared powder specimens. The nearly flattened tetrahedral geometry prevails for  $\text{CuO}_4$  in the near surface regions of the particles whereas square planar  $\text{CuO}_4$  groups are dominant in the interior regions of the nano particles. The powders derived from the oxalate precursor have excellent sinterability resulting in high density ceramics which exhibited giant dielectric constants upto 40000 (1 kHz) at 25°C accompanied by low dielectric loss  $< 0.07$ )

**7) Chiodelli et al. [35]** He investigated about the electric and dielectric properties of pure and doped CCTO perovskite materials. Where, AC impedance spectroscopy measurements were performed in the temperature range 15-700 K on pure and Ni, Fe and Co doped CCTO materials. The Capacitance values were also confirmed by direct current measurements at room temperature. Thermoelectric power measurements showed that the electrons are involved in the conduction process of the semiconducting bulk region. The IS results evidenced a dielectric

behaviour in the region of grain boundary and giving a permittivity of about 3400 for the pure sample hence CCTO can be considered an internal barrier layer capacitance (IBLC) material. The giant permittivity value of CCTO can be strongly increased to values of  $15 \times 10^4$  by Co doping on Ti site. The IBLC behaviour together with the giant permittivity and the opportunity to combine resistance and capacitance values in parallel circuit with evidence the applicability of this material as an integrated resonant element for the electronic industry.

8) *Tselev et al.* [36] reported about the dielectric response of CCTO thin films grown epitaxially on LaAlO<sub>3</sub> (001) substrates with pulsed laser deposition. The dielectric response of the films were found to be strongly dominated by a power law in frequency typical of materials with localized hopping charge carriers in contrast to the Debye like response of the bulk material. The film conductivity decreases by annealing in oxygen and it suggests that oxygen deficit was a cause of the relatively high film conductivity. With increase of the oxygen content at room temperature frequency response of the CCTO thin films changes from the response indicating the presence of some relatively low conducting capacitive layers to purely power law and then toward a frequency independent response with a relative dielectric constant  $\epsilon_r' = 10^2$ . The film conductance and dielectric response decrease upon decrease of the temperature with dielectric response being dominated by the power law frequency dependence. The dielectric response of the films below 80k was frequency independent with  $\epsilon_r'$  close to  $10^2$ . The results provide another piece of evidence for an extrinsic Maxwell Wagner type origin of the colossal dielectric response of the bulk CCTO material connected with electrical inhomogeneity of the CCTO bulk materials.

9) *K D Mandal et al.* [37] The effect of Co<sup>+2</sup> doping on Cu<sup>+2</sup> and Ti<sup>+4</sup> sites in calcium copper titanate, CaCu<sub>3</sub>Ti<sub>4</sub>O<sub>12</sub>, has been examined. The doped compositions, CaCu<sub>3-x</sub>Co<sub>x</sub>Ti<sub>4</sub>O<sub>12</sub> and CaCu<sub>3</sub>Ti<sub>4-x</sub>Co<sub>x</sub>O<sub>12</sub> ( $x = 0-10$ ) ceramics, were prepared by novel semi-wet route. In this method, calcium, copper and cobalt salts were taken in solution form and TiO<sub>2</sub> was used in solid form. XRD analysis confirmed the formation of single-phase materials. Structure of CaCu<sub>3</sub>Ti<sub>4</sub>O<sub>12</sub> does not change on doping with cobalt either on Cu-site or Ti-site and it remains cubic. Scanning electron micrographs (SEM) show average grain size of CaCu<sub>2.9</sub>Co<sub>0.1</sub>Ti<sub>4</sub>O<sub>12</sub> to be larger than CaCu<sub>3</sub>Ti<sub>3.9</sub>Co<sub>0.1</sub>O<sub>12</sub> ceramic. Energy dispersive X-ray spectroscopy (EDX) studies confirmed the purity of parent and Co-doped CaCu<sub>3</sub>Ti<sub>4</sub>O<sub>12</sub> ceramics. Dielectric constant ( $\epsilon_r$ ) and dielectric loss ( $\tan \delta$ ) of CaCu<sub>2.9</sub>Co<sub>0.1</sub>Ti<sub>4</sub>O<sub>12</sub> is comparatively higher than that of CaCu<sub>3</sub>Ti<sub>3.9</sub>Co<sub>0.1</sub>O<sub>12</sub> ceramic at all measured frequencies and temperatures.

10) *Chivalrat Masingboon et al.* [38] nano sized powders of CCTO were synthesized by a polymerized complex method and calcined at 600, 700 and 800°C in air for 8 h.

The diameter of the powders ranges from 30 to 100 nm. The CCTO powders were characterized by TG-DTA, XRD, FTIR, SEM and TEM. Sintering of the powders was conducted in air at 1100°C for 16 h. The XRD results indicated that all sintered samples have a typical perovskite CCTO structure with some amount of CaTiO<sub>3</sub> and CuO. SEM micrographs of the sintered CCTO ceramics showed the average grain size of 10-15µm. The samples exhibit a giant dielectric constant  $\epsilon_r'$  of 10000–20000. It is found that  $\epsilon_r$  is independent on the frequency and weakly dependent on temperature. The Maxwell Wagner polarization mechanism is used to explain the high permittivity in these ceramics. It is also found that all three sintered samples have the same activation energy of grains which is 0.116 eV. On the other hand the activation energy of grain boundaries is found to be 0.219, 0.391 and 0.641 eV for CCTO ceramics prepared using the CCTO powders calcined at 600, 700 and 800°C, respectively.

### **3. Objective**

#### **The objective of this project is:**

1. Preparation of CCTO powder by conventional solid state route.
2. Characterization of the prepared powder.
3. Characterization of the CCTO pellets to obtain high dielectric constant for capacitor application.

### **4. Calculations**

For starting powders



For the preparation of 15 grams of CCTO; the amount of the raw material are taken as follows.



<b>SAMPLES USED</b>	<b>MOLECULAR WEIGHT</b>	<b>QUANTITY</b>
a) CaO	56.0774g/mol	1.3692 grams
b) CuO	79.545g/mol	5.8268 grams
c) TiO <sub>2</sub>	79.90g/mol	7.8038 grams

These raw materials were first mixed thoroughly using agate mortar for different milling time 20, 25 and 30 hour to prepared three samples so as to form a fine mixture of the mixed powders. The powder obtained after grinding was greyish in appearance which change dark brown after calcinations.

## **CHAPTER-3**

---

### **CHARACTERIZATION TECHNIQUE**

### 3.1.1 X- ray diffraction

X ray diffraction (XRD) is a material characterization technique that can be useful for analyzing the lattice structure of a material. XRD is a non destructive method for the structure analysis of crystals. The sample is irradiated with monochromatic X ray light and the stray radiation recorded. An important field of application is the identification of crystalline fractions in powders. The X-ray radiation most commonly used is that emitted by copper whose characteristic wavelength for the K radiation is  $1.5418 \text{ \AA}$ . When the incident beam strikes powder sample diffraction occurs in every possible orientation of  $2\theta$ . The diffracted beam may be detected by using a moveable beam detector. Such as a Geiger counter which is connected to a chart recorder. In normal use the counter is set to scan over a range of  $2\theta$  values at a constant angular velocity. The routinely a  $2\theta$  range of 5 to 80 degrees is sufficient to cover the most useful part of the powder pattern. The scanning speed of the counter is usually  $2\theta$  of 20/min and thus about 30 minutes are needed to obtain a trace.

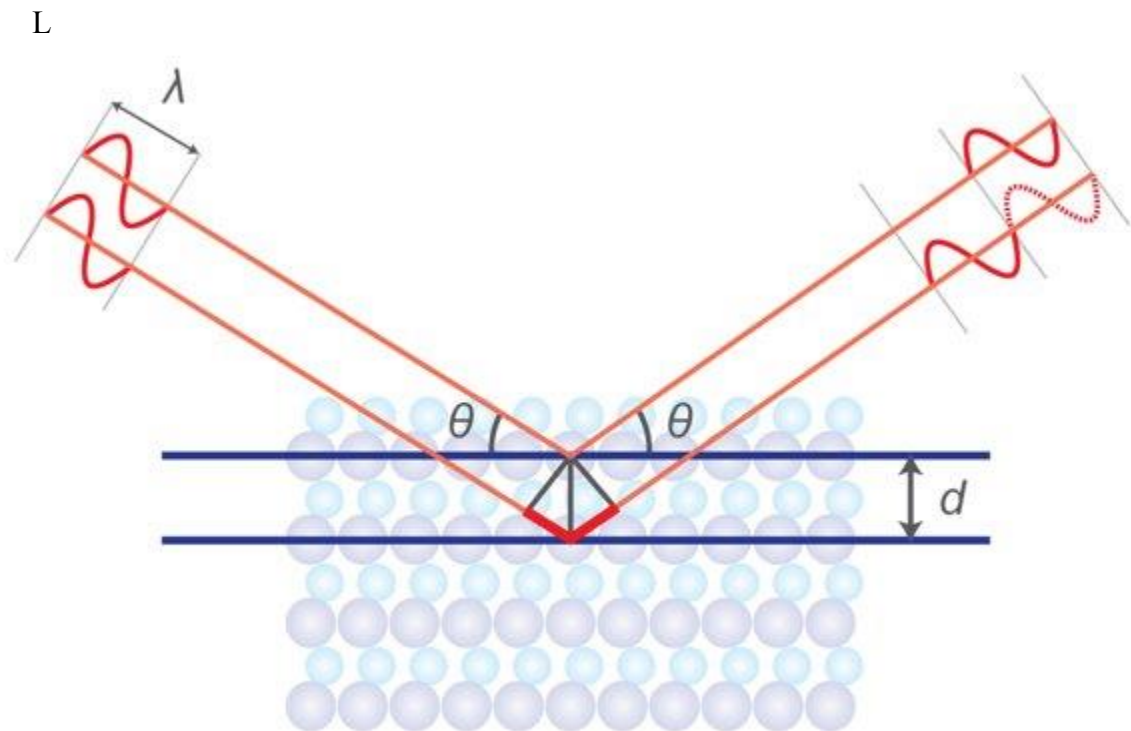


Figure 3.1 Basic process of XRD

### 3.1.2 Features

1. X ray measurements of powders are easily performed; they non destructive and only small quantities (approx. 2 mg) are needed.

The samples may be of different form

- Powder in capillaries in transmission
- Plane -parallel pieces in reflection
- Powder between foil in transmission
- Layers on substrate in reflection

2. The Bulk samples must have particular dimensions, they must be parallel plane and smooth, amorphous fractions are not analysed.

3. Crystallite sizes between 20 and 100<sup>0</sup>A can be calculated from the half widths according to the Scherrer's formula.

4. Lattice constants can be refined to determine e.g. stoichiometries according to the Vegard formula.

5. Structure controls and structure determinations can be performed with the Rietveld program.

6. Simple texture measurements of layers on substrates can be rapidly carried out using position sensitive detectors.

### 3.1.3 Basic principles of XRD

XRD analysis uses the property of crystal lattices to diffract monochromatic X-ray light. This involves the occurrence of interferences of the waves scattered at the successive planes which are described by Bragg's equation:

Diffraction occurs only when Bragg's Law is satisfied for constructive interference from planes with spacing  $d$ . The inter planer spacing calculated from

$$\text{Bragg's Law } n\lambda = 2d\sin\theta$$

(Where 'n' is any integer, 'λ' is the x-ray wave length, 'θ' is the Bragg's angles 'd' is the inter planer spacing).

Determining the particle size or grain size:

The mean crystalline sizes of the powders are calculated using Scherrer's formula

$$D = 0.9 \lambda / \beta \cos\theta,$$

Where D is average crystallite size  $\lambda = 1.541 \text{ \AA}$  (X-ray wavelength),

$$\beta = B - b$$

, B being the width of the diffraction peak at half maximum for the diffraction angle  $2\theta$ , b is calculated from the peak width of single crystal silicon wafer.

### Peak Width - Full Width at Half Maximum (FWHM)

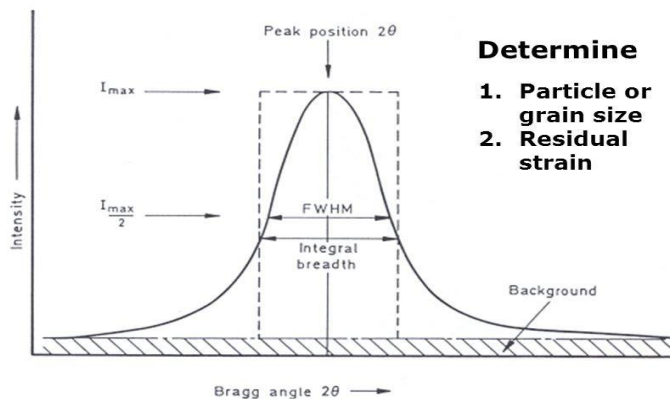


Fig.3.2 X-ray diffraction peak to measure the FWHM

- In diffractograms of powders not free from phase shift several diffraction patterns of different crystalline fractions can be superimposed. The detector is a position sensitive proportional counter for high speed recording or a scintillation counter for better angular resolution. Instruments that work on this principle are called diffractometers.
- By accurately measuring peak positions over a long range of  $2\theta$ , you can determine the unit cell lattice parameters of the phases in your sample
- Sealed X ray tubes tend to operate at 1.8 to 3 kW.
- The unit cell is the basic repeating unit that defines a crystal.



**Fig.3.3 XRD apparatus**

### 3.2.1 SEM Analysis

A scanning electron microscope (SEM) is a type of electron microscope that produces images of a sample by scanning it with a focused beam of electrons. In the sample the electrons interact with electrons and produces signals that can be detected and gives information about the sample's surface topography and its composition. The beam of the electron is scanned in a pattern named as raster scan. Here the beam's position is combined with the detected signal to produce an effective image. The resolution obtained is about 1 nanometer can be achieved by SEM.

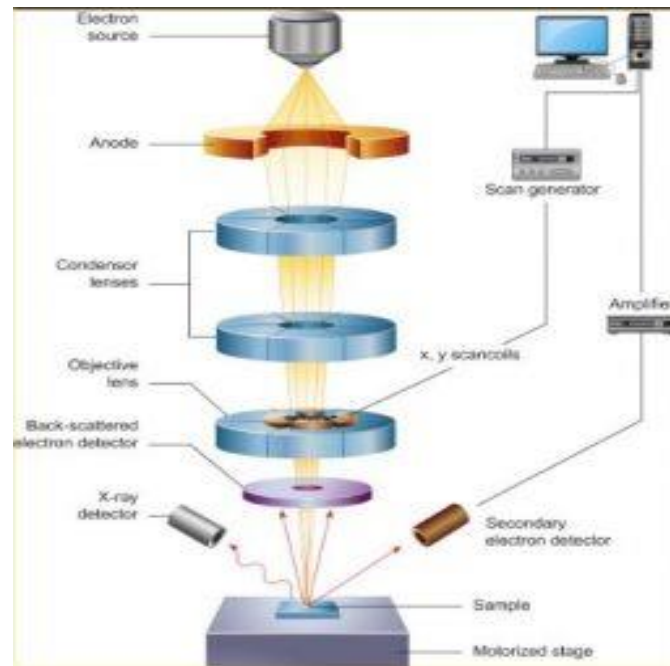


**Figure 3.4 Basic Components of SEM**

### **3.3 Field-emission Scanning Electron Microscope (FESEM):**

#### **Principle**

Under vacuum, electrons generated by a Field Emission Source are accelerated in a field gradient. The beam passes through Electromagnetic Lenses, focusing onto the specimen. As result of this bombardment different types of electrons are emitted from the specimen. A detector catches the secondary electrons and an image of the sample surface is constructed by comparing the intensity of these secondary electrons to the scanning primary electron beam. Finally the image is displayed on a monitor. A FESEM is used to visualize very small topographic details on the surface or entire or fractioned objects. Researchers in biology, chemistry and physics apply this technique to observe structures that may be as small as 1 nanometer (= billion of a millimeter). The FESEM may be employed for example to study organelles and DNA material in cells, synthetically polymers, and coatings on microchips.



**Fig.3.5** FESEM apparatus



- **Preparation**

In order to be observed with a SEM/FESEM non metallic specimens are first made conductive for current. This is done by coating them with an extremely thin layer (1.5 - 3.0 nm) of gold or gold palladium. Further on, objects must be able to sustain the high vacuum and should not alter the vacuum, for example by losing water molecules or gasses. Metals, polymers and crystals are usually not problematic and keep their structure in the SEM/FESEM. Biological material, however, requires a prefixation, e.g. with cold slush nitrogen (cryo-fixation) or with chemical compounds. This particular microscope is forseen of a special cryo-unit where frozen objects can be fractured and coated for direct observation in the FESEM. Chemically fixed material needs first to be washed and dried below the critical point to avoid damage of the fine structures due to surface tension. Coating is then performed in a separate device.

- **Source of electrons**

In standard electron microscopes electrons are mostly generated by heating a tungsten filament by means of a current to a temperature of about 2800°C. Sometimes electrons are produced by a crystal of lanthanumhexaboride (LaB6) that is mounted on a tungsten filament. This modification results in a higher electron density in the beam *81* and a better resolution than with the conventional device. In a field emission (FE) scanning electron microscope no heating but a "cold" source is employed. An extremely thin and sharp tungsten needle (tip diameter 10– 7 –10-8 m) functions as a cathode in front of a primary and secondary anode. The voltage between cathode and anode is in the order of magnitude of 0.5 to 30 KV. Because the electron beam produced by the FE source is about 1000 times smaller than in a standard microscope, the image quality is markedly better. As field emission necessitates an extreme Vacuum (10-8 Torr) in the column of the microscope, a device is present that regularly decontaminates the electron source by a current flash. In contrast to a conventional tungsten filament, a FE tip last theoretically for a lifetime, provided the vacuum is maintained stable. Field emission necessitates an extreme Vacuum (10-8 Torr) in the column of the microscope, a device is present that regularly decontaminates the electron source by a current flash. In contrast to a conventional tungsten filament, a FE tip last theoretically for a lifetime, provided the vacuum is maintained stable.

- **Image formation**

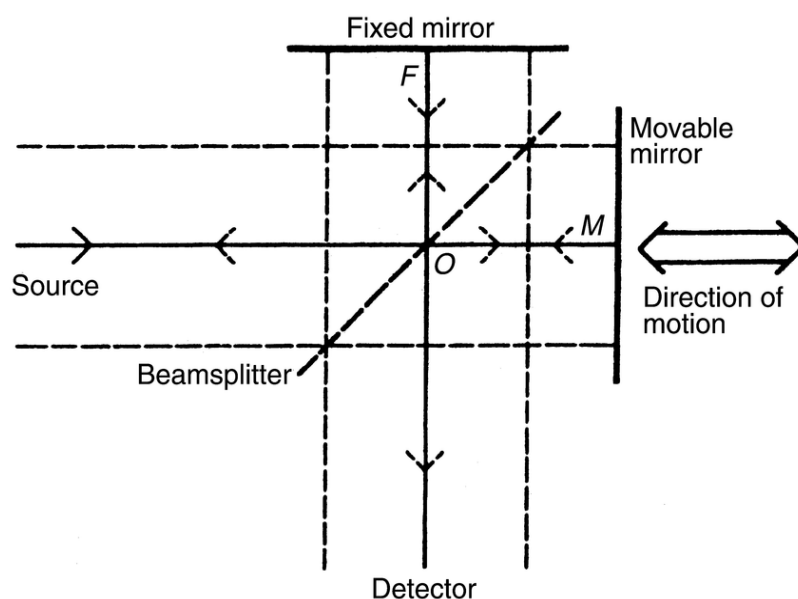
When the primary probe bombards the object, secondary electrons are emitted from the object surface with a certain velocity that is determined by the levels and angles at the surface of the object. The secondary electrons, which are attracted by the Corona, strike the scintillator (fluorescing mirror) that produces photons. The location and intensity of illumination of the mirror vary depending on the properties of the secondary electrons. The signal produced by the scintillator is amplified and transduced to a video signal that is fed to a cathode ray tube in synchrony with the scan movement of the electron beam. The contrast in the real time image that appears on the screen reflects the structure on the surface of the object. Parallel to the analogy image, a digital image is generated which can be further processed.

### **3.4 Fourier Transform Infrared Spectroscopy (FTIR):**

Fourier Transform Infrared Spectroscopy (FTIR) is a technique which is used to analyze the chemical composition of many organic chemicals, polymers, paints, coatings, adhesives, lubricants, semiconductor materials, coolants, gases, biological samples, inorganic and minerals. FTIR can be used to analyze a wide range of materials in bulk or thin films, liquids, solids, pastes, powders, fibers, and other forms. FTIR analysis can give not only qualitative (identification) analysis of materials, but with relevant standards, can be used for quantitative (amount) analysis. FTIR can be used to analyze samples up to ~11 millimeters in diameter, and either measure in bulk or the top ~1 micrometer layer. An FTIR Spectrometer is an instrument which acquires broadband NIR to FIR spectra. Unlike a dispersive instrument, i.e. grating monochromator or spectrograph, and FT-IR Spectrometer collects all wavelengths simultaneously. An FT-IR (Fourier Transform Infra-Red) is a method of obtaining infrared spectra by first collecting an interferogram of a sample signal using an interferometer, and then performing a Fourier Transform (FT) on the interferogram to obtain the spectrum. An FTIR Spectrometer collects and digitizes the interferogram, performs the FT function, and displays the spectrum.

- **Principle of operation:**

An FTIR is typically based on a Michelson Interferometer the interferometer consists of a beam splitter, a fixed mirror, and a mirror that translates back and forth, very precisely. The beam splitter is made of a special material that transmits half of the radiation striking it and reflects the other half. Radiation from the source strikes the beam splitter and separates into two beams. One beam is transmitted through the beam splitter to the fixed mirror and the second is reflected off the beam splitter to the moving mirror. The fixed and moving mirrors reflect the radiation back to the beam splitter. Again, half of this reflected radiation is transmitted and half is reflected at the beam splitter, resulting in one beam passing to the detector and the second back to the source.



A beam of infrared light (wavelength  $\sim 0.7\text{-}500 \mu\text{m}$ ) is focused on the samples using all reflected optics. Depending on the sample composition, differing amounts of light are absorbed at different wavelengths. This pattern of light absorption is unique for almost every organic compound (except optical isomers) and many inorganic compounds. From the pattern of light absorbed, identification of the composition (qualitative analysis) can be made. With additional control over the sample thickness or sampling depth, the intensity of the individual absorbing components can be used to perform quantitative analysis (amount of each compound present).

User-provided reference samples aid in positive substance identification and compositional verification. FTIR can be used to identify chemicals from spills, paints, polymers, coatings, drugs, and contaminants. FTIR is perhaps the most powerful tool for identifying types of chemical bonds (functional groups). The wavelength of light absorbed is characteristic of the chemical bond as can be seen in this annotated spectrum. A Shimadzu IRPrestige-21 FTIR spectrometer was used to record the spectra in the mid IR region, (i.e. 400-4000  $\text{cm}^{-1}$ ) as shown in figure below.



**Fig. 3.5** Shimadzu IRPrestige-21 FTIR spectrometer

### 3.7 Dielectric Spectroscopy

An LCR meter is used for the measurement of electrical properties including capacitance ( $C_s$ ), loss tangent ( $\tan\delta$ ), resistance component ( $R_x$ ) and reactance component ( $X_x$ ) and subsequently from these values dielectric constant ( $\epsilon_r$ ) of the sample can be determined.

It works on the principle of auto balancing bridge method, where the sample is placed in a bridge and the impedance  $Z_1$  and  $Z_2$  being known, the value of  $Z_3$  is changed until no current flows through the terminals of  $D$ . Then the impedance value of sample ( $Z_s$ ) is calculated by  $Z_s = (Z_2 Z_3)/Z_1$ . Subsequently, the values of  $R_x$  and  $X_x$  can be calculated from the impedance value and from those  $C_s$  and  $\tan\delta$ , values are calculated. The values of  $C_s$ ,  $R_x$ ,  $X_x$ , ( $\tan\delta$ ) are displayed by the instrument. To measure the desired values, the material is first pressed into circular pellets followed by application of silver paste on both surfaces to provide electrical contacts and finally, electrodes are connected to it.  $\epsilon_r$  is calculated from the capacitance value by  $\epsilon_r = (C_s d)/(A \epsilon_0)$ , where  $d$  is the thickness of the pellets,  $A$  is the area of the metalized portion of one surface and  $\epsilon_0$  is  $8.854 \times 10^{-12}$  F/m.

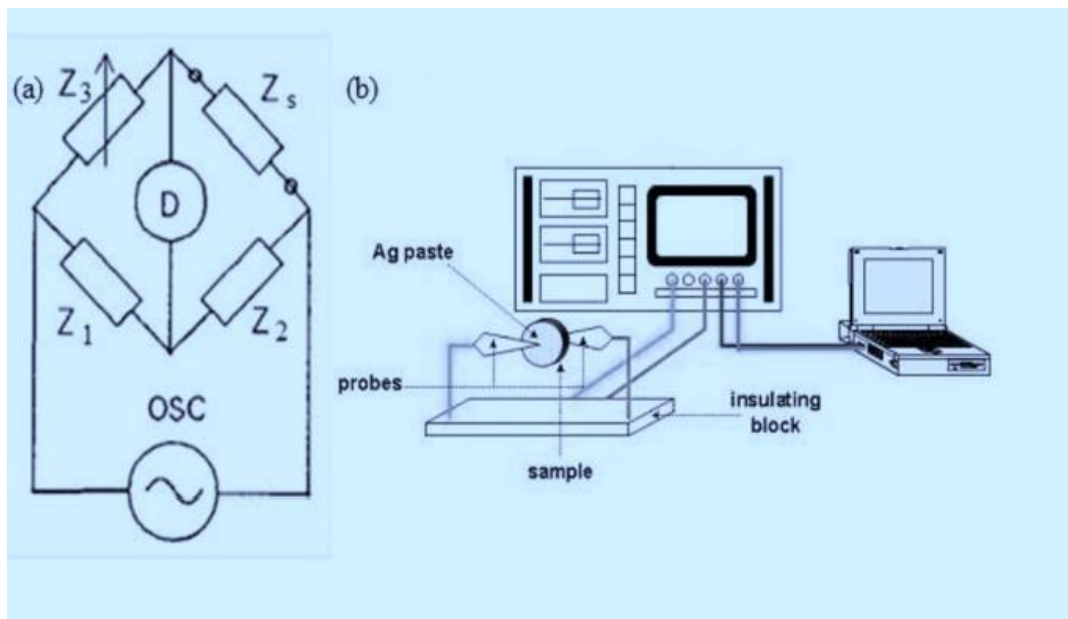


Figure 3.7 a) auto balancing bridge b) a typical LCR meter setup

## **CHAPTER-4**

---

### **EXPERIMENTAL WORK**

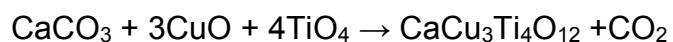
## 4. EXPERIMENTAL WORK

### 4.1 PREAMBLE

In this section the detailed experimental procedure for the study of  $\text{CaCu}_3\text{Ti}_4\text{O}_{12}$  (CCTO) synthesis has been discussed by modified solid state route. The amounts and ratio of the  $\text{CaCO}_3$ ,  $\text{CuO}$  and  $\text{TiO}_2$  (AR Grade, Lobe India) used for preparing the different batches in certain ratio were taken based on stoichiometry and scientific research survey. Stoichiometric used for precursor powder is 1:3:4. We will compare the characteristics of calcium copper titanate with different milling time (agate mortar) at same temperature.

### EXPERIMENTAL PROCEDURE

**The main reaction as per stoichiometric relation is shown:**

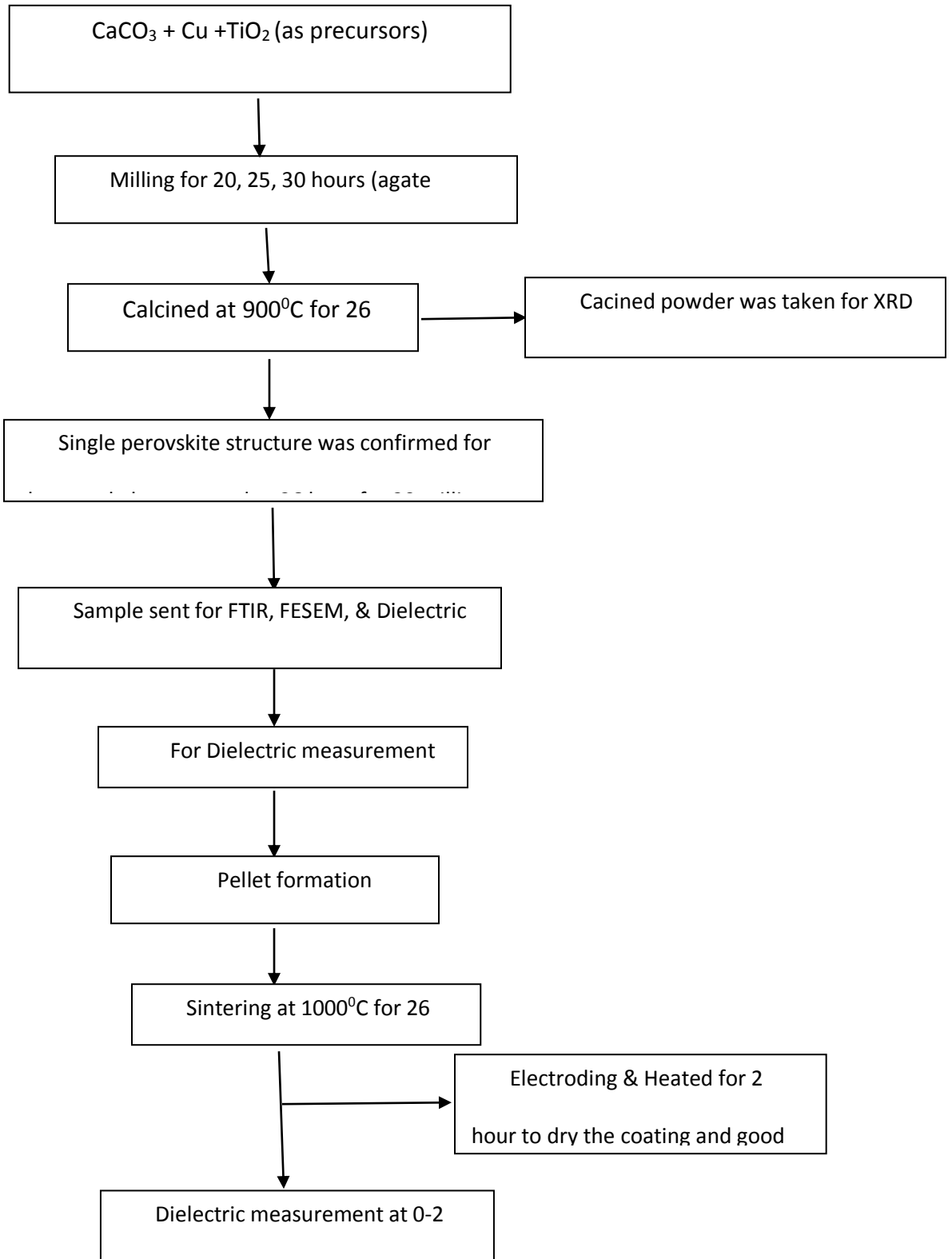


Following steps involved for synthesis of this compound are given below:

- 1)  $\text{CaO}$  (calcium oxide),  $\text{CuO}$  (copper oxide) and  $\text{TiO}_2$  (titanium dioxide) were taken in stoichiometric ratio to prepare  $\text{CaCu}_3\text{Ti}_4\text{O}_{12}$ . The raw materials were measured using the high precision balance correct up to 4 decimal places.
- 2) The mixed sample was taken out and after it got dry it was thoroughly grounded in agate mortar for preparing three different samples with different milling time as 20,25,and 30 hours respectively so as to obtain a mixed powder of the raw materials.
- 3) The grounded sample was taken in an alumina crucible and calcined at  $900\text{ }^\circ\text{C}$  for 26 hours with rate  $5^\circ\text{C}/\text{min}$  followed by furnace cooling.

- 4) The mixtures were taken out after the temperature came down to room temperature.
- 5) Phase formation of CCTO was confirmed through X-ray diffraction analysis using powder diffractometer (RIGAKU ULTIMA, PW 3020)
- 6) Single perovskite phase was confirmed from XRD analysis for the sample calcined for 30 hour milling at 900°C.
- 7) The calcined samples at 900°C for 26 hour with 30 hour milling time was chosen and sent for SEM, FESEM and FTIR analysis.
- 8) The calcined sample at 900 °C for 26 hour was chosen and mixed with polyvinyl alcohol that acts as a binder. After mixing the binder the sample is left for sometime so that the mixture dries and then grinded again.
- 9) The sintered powder mixture poured into a 12mm diameter mould cavity in a die system. The entire die system was placed in a manually operated hydraulic pressing machine. Pressing were performed by applying an uniaxial pressure about 60 kg/cm<sup>2</sup>. Thus Cylindrical pellets of CCTO were obtained.
- 10) The CCTO pellets were sintered in an indigenous programmable conventional furnace at 900°C for 26 hour in normal atmosphere.
- 11) The sintered pellets were coated with silver paste and heated for 1 hour to dry the coating and for good adhesion.
- 12) The dielectric measurement was then made at 1 kHz 10 kHz 100 kHz and 1 MHz.





## **CHAPTER-5**



### **RESULT & DISCUSSION**

## 5. RESULT & DISCUSSION

### 5.1 XRD ANALYSIS OF SYNTHESIS OF CCTO

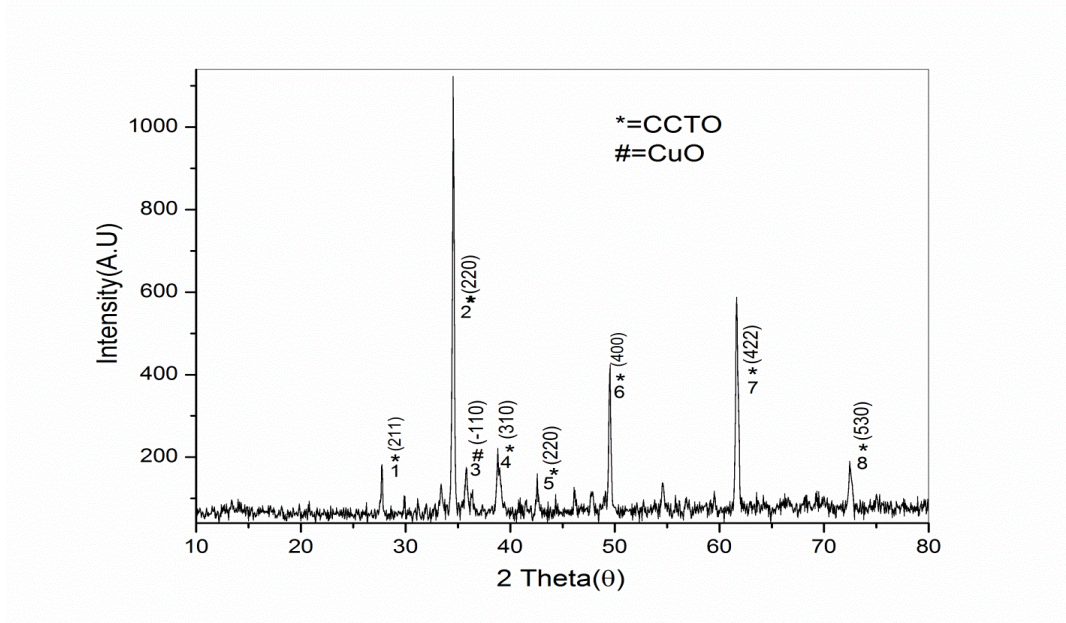


Fig5.1.1 (a) XRD of CCTO treated for 20 hour milling and 26 hour heating at 900

#### 1.1 CTTO 20 hour milling and 26 hour heating.

Peak No	d-value of corresponding peak	2θ value of corresponding peak	Standard d-value	Planes	Chemical formula of compound	JCPDS Card No	Crystalline size(using schhere's formula)
1	3.2121	27.750	3.2284	(220)	TiO	85-2084	
2	2.5939	34.550	2.6138	(220)	CaCu <sub>3</sub> Ti <sub>4</sub> O <sub>12</sub>	75-1149	82.47nm
3	2.5061	35.800	2.52	(-110)	CuO	01-080-1916	
4	2.3190	38.800	2.3378	(310)	CaCu <sub>3</sub> Ti <sub>4</sub> O <sub>12</sub>	75-1149	124.53nm
5	2.1205	42.600	2.1341	(222)	CaCu <sub>3</sub> Ti <sub>4</sub> O <sub>12</sub>	75-1149	
6	1.8399	49.500	1.8482	(400)	CaCu <sub>3</sub> Ti <sub>4</sub> O <sub>12</sub>	75-1149	129.34nm
7	1.5032	61.650	1.5090	(422)	CaCu <sub>3</sub> Ti <sub>4</sub> O <sub>12</sub>	75-1149	68.68nm
8	1.2610	75.300	1.2678	(530)	CaCu <sub>3</sub> Ti <sub>4</sub> O <sub>12</sub>	75-1149	

Fig 5.1.1 (a) shows the XRD pattern of the CCTO with 20 hour milling followed by heat treatment at 900°C for 26 hour. The XRD patterns confirm the single phase structure. At this composition we get sharp peaks in the  $2\theta$  range at 34.55°, 38.8°, 49.50° and 61.65°. Small peaks can also be seen around 27.75°, 35.80°, 42.60° and 75.30° respectively. The peaks are indexed as per the (hkl) values reported in JCPDS file (75-1149). Appearance of peaks corresponding to CCTO phase indicated formation of single phase compound. Some impurities can also be detected like copper oxide peaks as per the (hkl) values reported in JCPDS file (78-1588) at 35.88°.

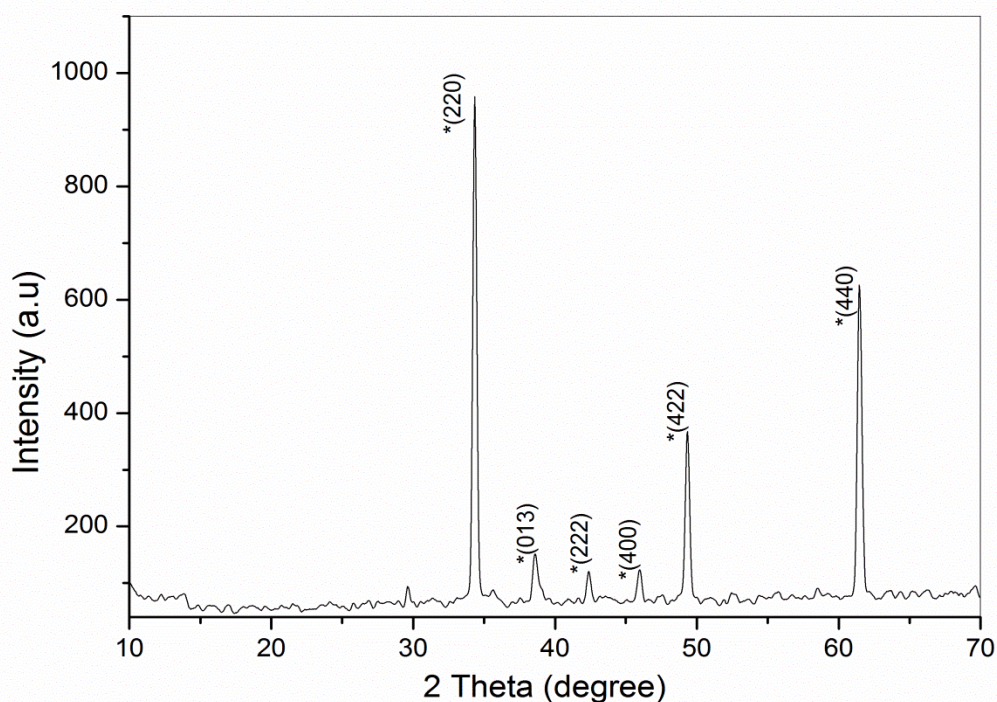


Fig 5.1.1(b) XRD of CCTO treated for 20 hour milling and 26 hour heating at 950°C

Peak No	d-value of corresponding peak	2θ value of corresponding peak	Standard d-value	planes	Chemical formula of compound	JCPDS Card No	Crystalline size(using scherrer's formula)
1	2.6122	34.300	2.6122	(220)	CaCu <sub>3</sub> Ti <sub>4</sub> O <sub>12</sub>	75-1149	122.92nm
2	2.3335	38.550	2.3335	(013)	CaCu <sub>3</sub> Ti <sub>4</sub> O <sub>12</sub>	75-1149	
3	2.1325	42.350	2.1325	(222)	CaCu <sub>3</sub> Ti <sub>4</sub> O <sub>12</sub>	75-1149	
4	1.8469	45.871	1.8469	(400)	CaCu <sub>3</sub> Ti <sub>4</sub> O <sub>12</sub>	75-1149	
5	1.5076	49.300	1.5076	(422)	CaCu <sub>3</sub> Ti <sub>4</sub> O <sub>12</sub>	75-1149	122.32nm
6	1.3066	61.450	1.3066	(440)	CaCu <sub>3</sub> Ti <sub>4</sub> O <sub>12</sub>	75-1149	145.41nm

Fig 5.1.1 (b) shows the XRD pattern of the CCTO with 20 hour milling followed by heat treatment at 950°C for 26 hour. The XRD patterns confirm the single phase structure at this composition we get sharp peaks in the 2θ range at 34.30°, 49.50° and 61.45°. Small peaks can also be seen around 38.55°, 42.35°, 42.35° respectively. The peaks are indexed as per the (hkl) values reported in JCPDS file (75-1149). Here it is observed that if temperature increased from 900°C to 950°C then impurities in copper oxide peaks removed and all peaks corresponding to CCTO phase indicated formation of single phase compound.

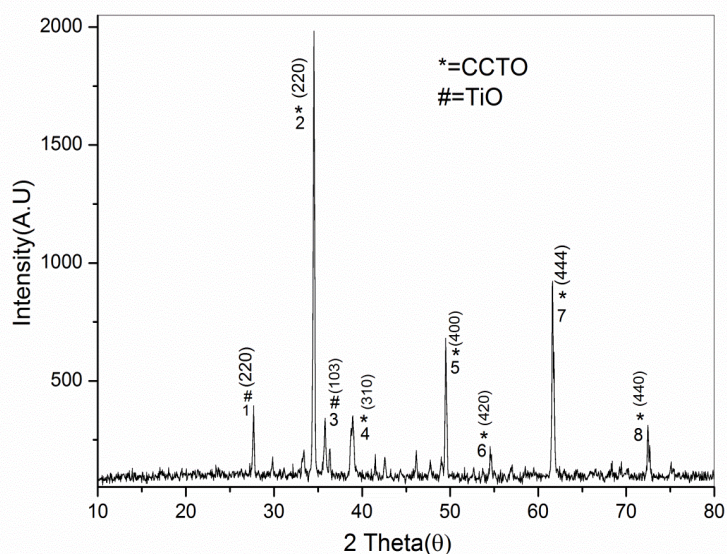


Fig 5.1.2(a) XRD of CCTO treated for 25 hour milling and 26 hour heating at 950°C.

### CCTO 25 hour milling and 26 hour heating

Peak No	d- value corresponding peak	2 $\theta$ value of corresponding peak	Standard d- value	Planes	Chemical formula	JCPDS Card No	Crystalline size(using scherrer's formula)
1	3.2235	27.650	3.2284	(220)	TiO	85-2084	
2	2.5975	34.500	2.6138	(220)	CaCu <sub>3</sub> Ti <sub>4</sub> O <sub>12</sub>	75-1149	122.99nm
3	2.4695	36.350	2.4283	(103)	TiO <sub>2</sub>	81-1286	
4	2.3219	38.750	2.3378	(310)	CaCu <sub>3</sub> Ti <sub>4</sub> O <sub>12</sub>	75-1149	
5	1.8399	49.500	1.8482	(400)	CaCu <sub>3</sub> Ti <sub>4</sub> O <sub>12</sub>	75-1149	86.71nm
6	1.6809	54.500	1.6531	(420)	CaCu <sub>3</sub> Ti <sub>4</sub> O <sub>12</sub>	75-1149	
7	1.5043	61.600	1.5090	(422)	CaCu <sub>3</sub> Ti <sub>4</sub> O <sub>12</sub>	75-1149	136.74nm
8	1.3034	72.490	1.3069	(440)	CaCu <sub>3</sub> Ti <sub>4</sub> O <sub>12</sub>	75-1149	145.60nm

Fig 5.1.2 (a) shows the XRD pattern of the CCTO with 25 hour milling followed by heat treatment at 900°C for 26 hour. The XRD patterns confirm the single phase structure. At this composition we get sharp peaks in the 2 $\theta$  range at 34.50°, 49.50°, 61.60° and 72.49°. Small peaks can also be seen around 36.35°, 38.75° and 54.50° respectively. The peaks are indexed as per the (hkl) values reported in JCPDS file (75-1149). Appearance of peaks corresponding to CCTO phase indicated formation of single phase compound. Some impurities can also be detected like titanium oxide peaks as per the (hkl) values reported in JCPDS file (78-1588) at 27.65°.

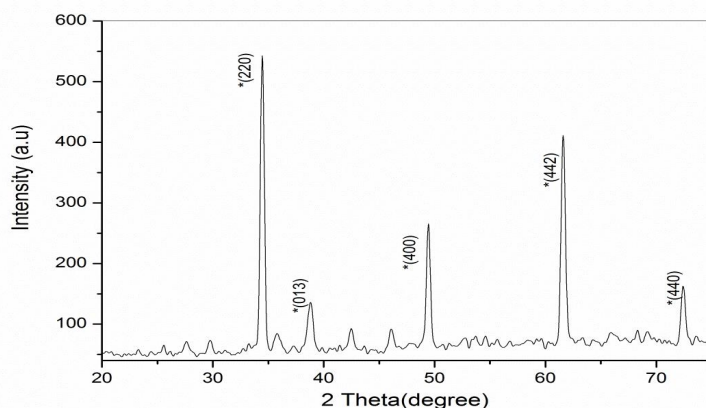


Fig 5.1.2 (b) XRD of CCTO treated for 25 hour milling and 26 hour heating at 950°C.



Peak No	d-value corresponding peak	2 $\theta$ value of corresponding peak	Standard d-value	Planes	Chemical formula	JCPDS Card No	Crystalline size(using scherrer's formula)
1	2.5975	34.50	2.6138	(220)	CaCu <sub>3</sub> Ti <sub>4</sub> O <sub>12</sub>	75-1149	122.92nm
2	2.3133	38.90	2.3378	(013)	CaCu <sub>3</sub> Ti <sub>4</sub> O <sub>12</sub>	75-1149	
3	1.8434	49.40	1.8482	(400)	CaCu <sub>3</sub> Ti <sub>4</sub> O <sub>12</sub>	75-1149	
4	1.5054	61.55	1.5090	(422)	CaCu <sub>3</sub> Ti <sub>4</sub> O <sub>12</sub>	75-1149	86.64nm
5	1.3050	72.35	1.3069	(440)	CaCu <sub>3</sub> Ti <sub>4</sub> O <sub>12</sub>	75-1149	145.41nm

Fig 5.1.1 (b) shows the XRD pattern of the CCTO with 20 hour milling followed by heat treatment at 950°C for 26 hour. The XRD patterns confirm the single phase structure. At this composition we get sharp peaks in the 2 $\theta$  range at 34.50°, 49.40° and 61.55°. Small peaks can also be seen around 38.90° and 72.35° respectively. The peaks are indexed as per the (hkl) values reported in JCPDS file (75-1149). Here it is observed that if temperature increased from 900°C to 950°C then impurities in titanium oxide peaks removed and all peaks corresponding to CCTO phase indicated formation of single phase compound.

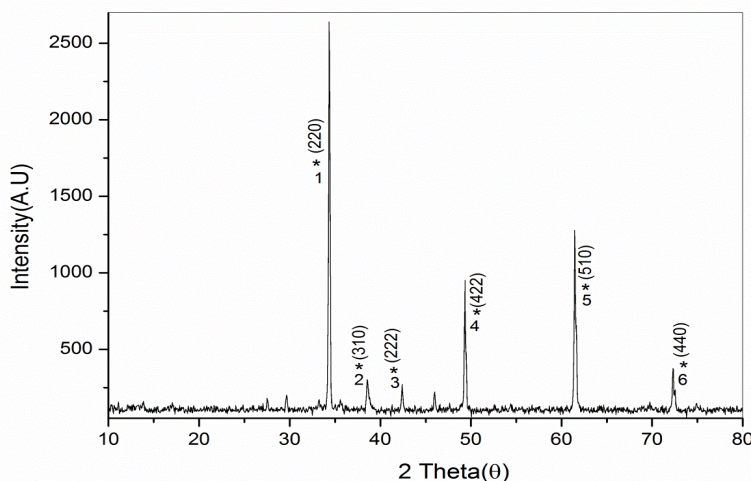
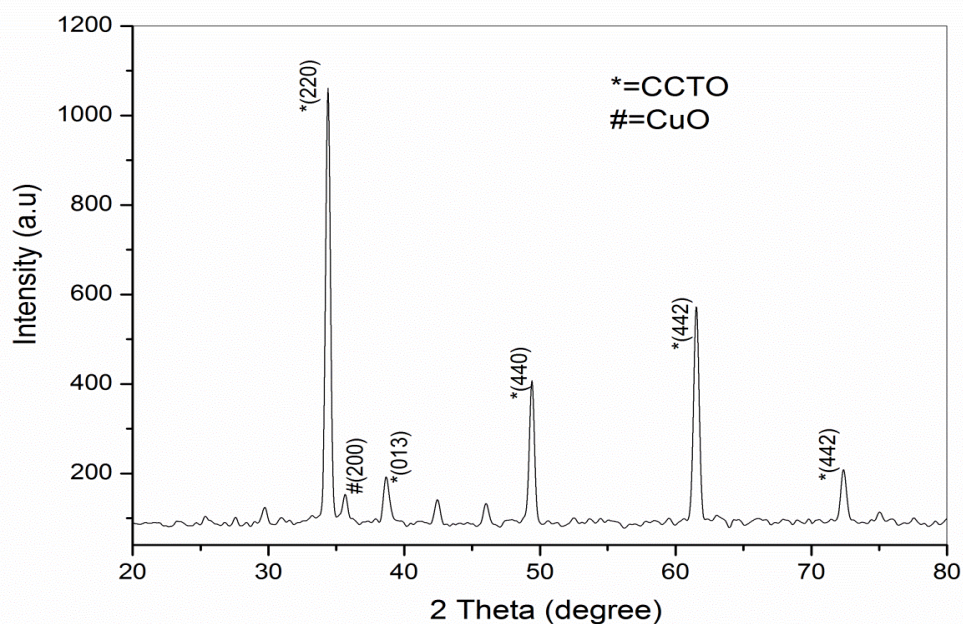


Fig 5.1.3 (a) CCTO 30 hour milling and 26 hour heating at 900°C

Peak No	d-value of corresponding peak	2 $\theta$ value of corresponding peak	Standard d-value	Planes	Chemical formula of compound	JCPDS Card No	Crystalline size(Using Scherrer's formula)
1	2.6085	34.350	2.6138	(220)	CaCu <sub>3</sub> Ti <sub>4</sub> O <sub>12</sub>	75-1149	82.66nm
2	2.3335	38.550	2.3378	(310)	CaCu <sub>3</sub> Ti <sub>4</sub> O <sub>12</sub>	75-1149	
3	2.1301	42.400	2.1341	(222)	CaCu <sub>3</sub> Ti <sub>4</sub> O <sub>12</sub>	75-1149	
4	1.8451	49.350	1.8482	(400)	CaCu <sub>3</sub> Ti <sub>4</sub> O <sub>12</sub>	75-1149	86.66nm
5	1.4395	64.700	1.4498	(510)	CaCu <sub>3</sub> Ti <sub>4</sub> O <sub>12</sub>	21-0140	
6	1.3058	72.300	1.3069	(440)	CaCu <sub>3</sub> Ti <sub>4</sub> O <sub>12</sub>	75-1149	97.52nm

Fig 5.1.3 (a) shows the XRD pattern of the CCTO with 25 hour milling followed by heat treatment at 900°C for 26 hour. The XRD patterns confirm the single phase structure. At this composition we get sharp peaks in the 2 $\theta$  range at 34.35°, 49.35° and 72.30°. Small peaks can also be seen around 38.55°, 42.40° and 64.70° respectively. The peaks are indexed as per the (hkl) values reported in JCPDS file (75-1149). Appearance of all peaks corresponding to CCTO phase indicated formation of single phase compound. But no impurities can be detected like titanium oxide and copper oxide peaks as per the (hkl) values reported in JCPDS file (78-1588).



5.1.3 (b) CCTO of 30 hour milling and 26 hour heating at 800°C

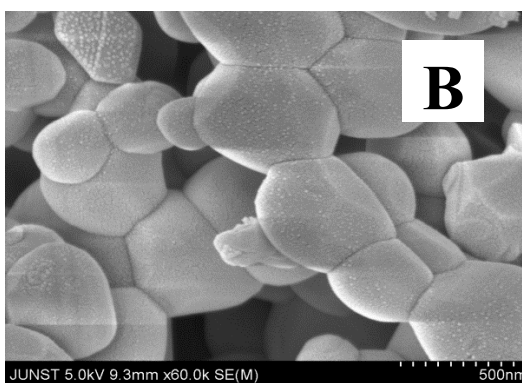
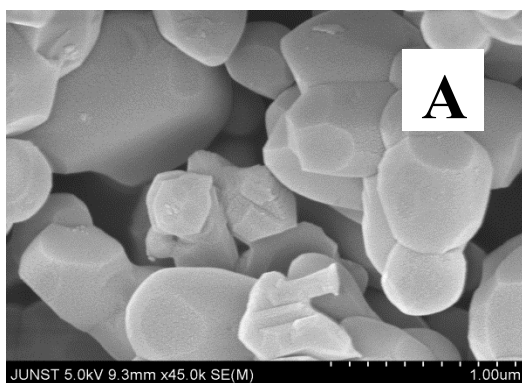


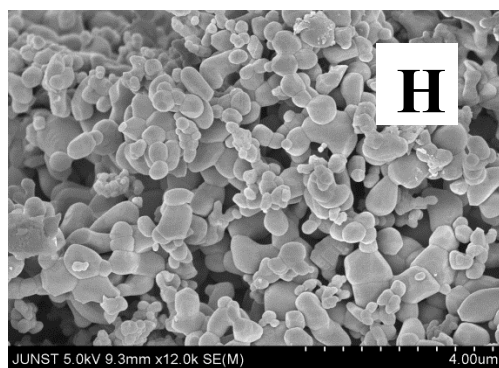
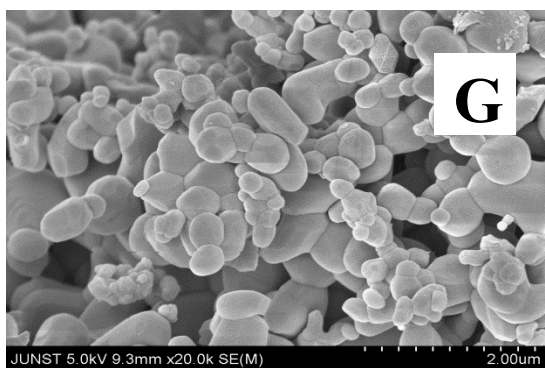
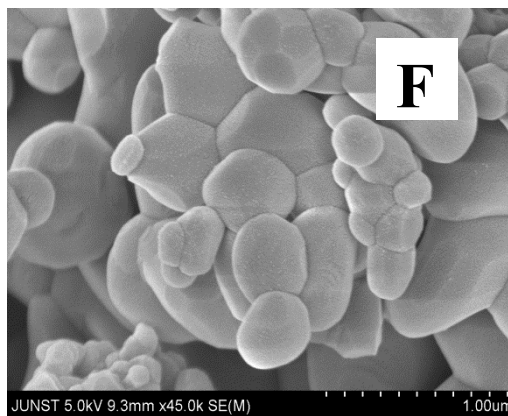
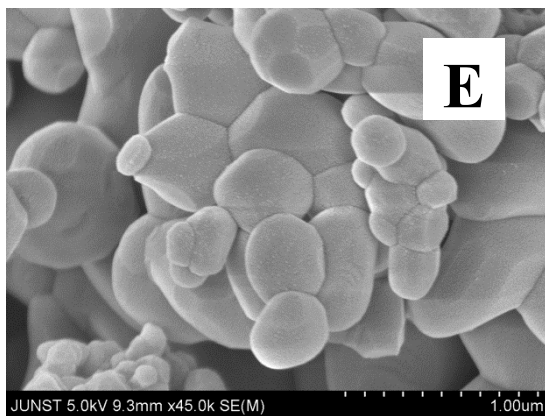
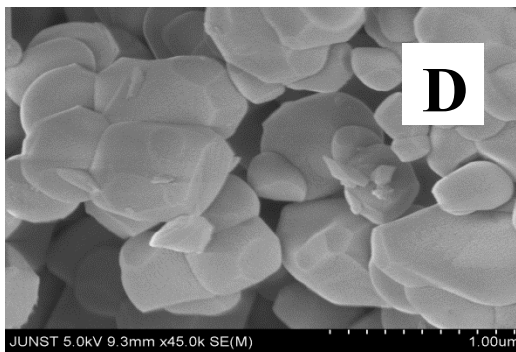
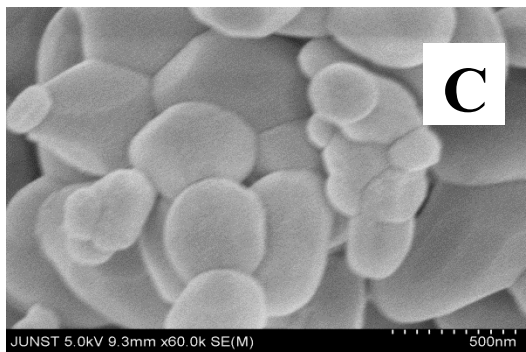
Peak No	d-value of corresponding peak	2 $\theta$ value of corresponding peak	Standard d-value	Planes	Chemical formula of compound	JCPDS Card No	Crystal line size(Using Scherrer's formula)
1	2.6049	34.400	2.6138	(220)	CaCu <sub>3</sub> Ti <sub>4</sub> O <sub>12</sub>	75-1149	61.73nm
2	2.5163	35.650	2.6138	(200)	CaCu <sub>3</sub> Ti <sub>4</sub> O <sub>12</sub>	75-1149	
3	2.3277	38.650	2.3378	(013)	CaCu <sub>3</sub> Ti <sub>4</sub> O <sub>12</sub>	75-1149	
4	1.8434	49.400	1.8482	(440)	CaCu <sub>3</sub> Ti <sub>4</sub> O <sub>12</sub>	75-1149	86.68m
5	1.5065	61.500	1.5090	(442)	CaCu <sub>3</sub> Ti <sub>4</sub> O <sub>12</sub>	75-1149	68.26nm
6	1.3050	72.350	1.3069	(440)	CaCu <sub>3</sub> Ti <sub>4</sub> O <sub>12</sub>	75-1149	

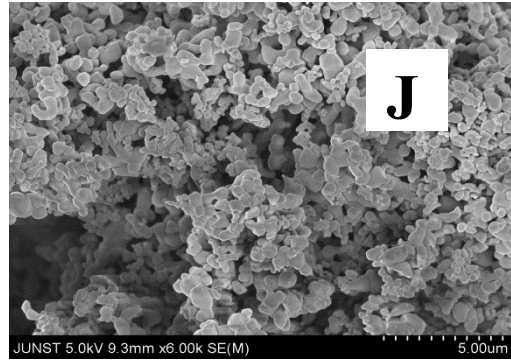
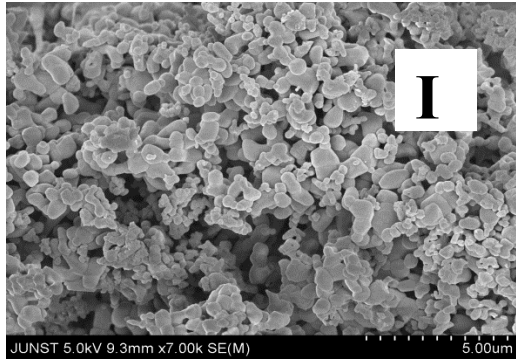
Fig 5.1.3 (b) shows the XRD pattern of the CCTO with 25 hour milling followed by heat treatment at 800°C for 26 hour. The XRD patterns confirm the single phase structure. At this composition we get sharp peaks in the 2 $\theta$  range at 34.40°, 49.35° and 72.35°. Small peaks can also be seen around 38.65° and 61.50° respectively. The peaks are indexed as per the (hkl) values reported in JCPDS file (75-1149). Appearance of all peaks corresponding to CCTO phase indicated formation of single phase compound. But some impurities can also be detected like copper oxide small peaks as per the (hkl) values reported in JCPDS files (81-1286)

## 5.2 FESEM ANALYSIS OF SYNTHESIS OF CCTO

The FESEM image for CCTO samples were taken and their grain size were calculated.





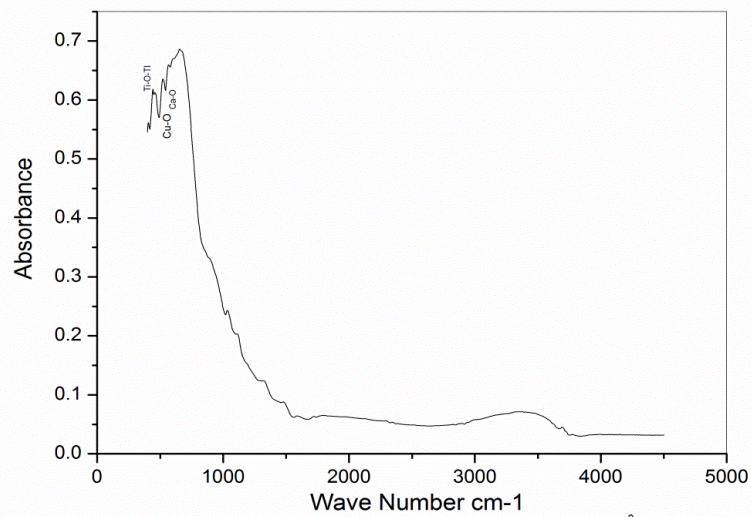


Figure

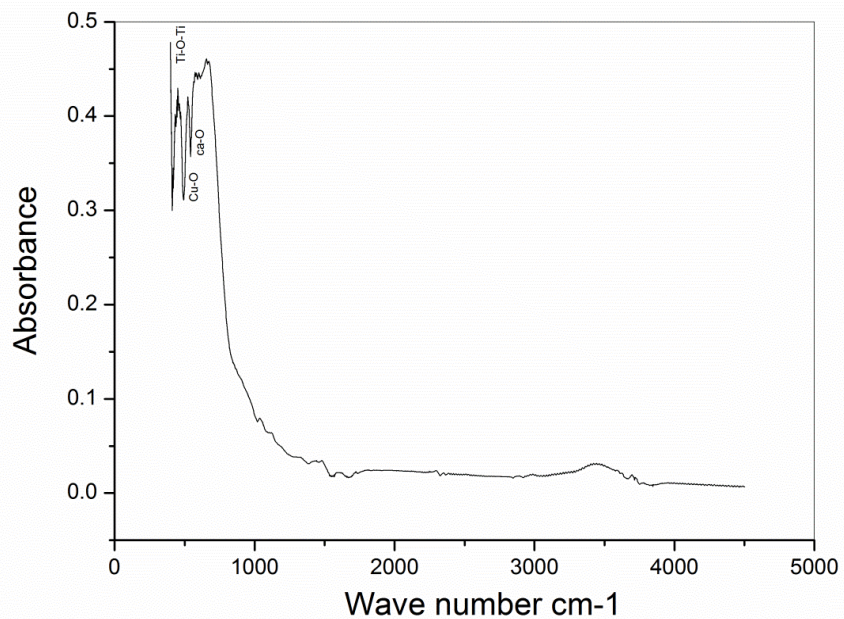
5.2.1 FESEM morphology of CCTO formed after 30 hour milling activation after soaking at 900<sup>0</sup>c for 26 hour at different magnification.

The FE-SEM Morphology of synthesized samples exhibit proper granular formation with strong agglomeration tendency. Few minute pores are noted within the agglomerate form. Strong interconnection among grains is noted. Grains are having spherical to irregular polygonal shape with conchoidal fracture face at top while some are having spherical shape. The smaller grains have size range from 40nm to 42nm. The bimodal distribution of grains that indicates the mechanochemical derived CCTO powder has hard agglomerates which on sintering from large grains. There is absence of any unwanted distortion observed in the matrix of the synthesise samples.

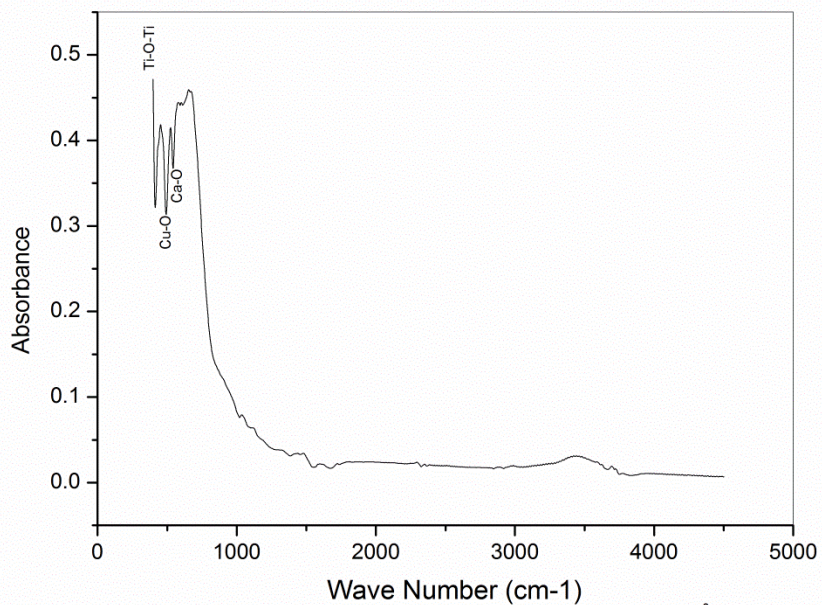
### 5.3 FTIR SPECTROSCOPY ANALYSIS OF CCTO.



5.3.1 FTIR of CCTO of 20 hour milling and heat treated at 900°C .



5.3.2 FTIR of CCTO of 25 hour milling and heat treated at 900°C

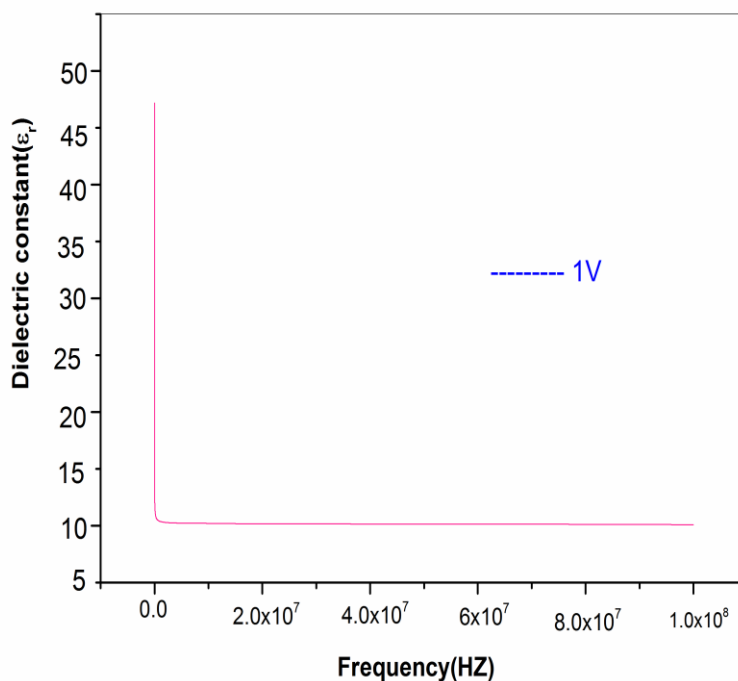


5.3.3 FTIR of CCTO of 30 hour milling and heat treated at 900°C

Wave number(cm-1)	Assignment
461 cm-1	Vibration mode of (Ti-O-Ti) band appeared [38].
524 cm-1	Cu-O bonding observed [39].
610 cm-1	Ca-O bonding observed [40]
370 cm-1 -700cm-1	Absorption band arising from mixed vibration of CuO <sub>4</sub> and TiO <sub>6</sub> group [41].

The figure 5.3 gives the IR spectra value for CCTO synthesized at 900<sup>0</sup>C for 26 hour with 25 hour milling. The main bond are available is mostly Ti-O-Ti, Cu-O, Ca-O and absorption bond arising from mixed vibration of CuO<sub>4</sub> and stretching at different molecular vibrations. Four major peaks is identify to show pure CCTO formation. Main M-O co-ordinations are noted in the range of 450cm<sup>-1</sup> to 620cm<sup>-1</sup>. The above result is in correspondence with the findings of previous researchers.

#### 5.4 DIELECTRIC PROPERTY ANALYSIS OF CCTO



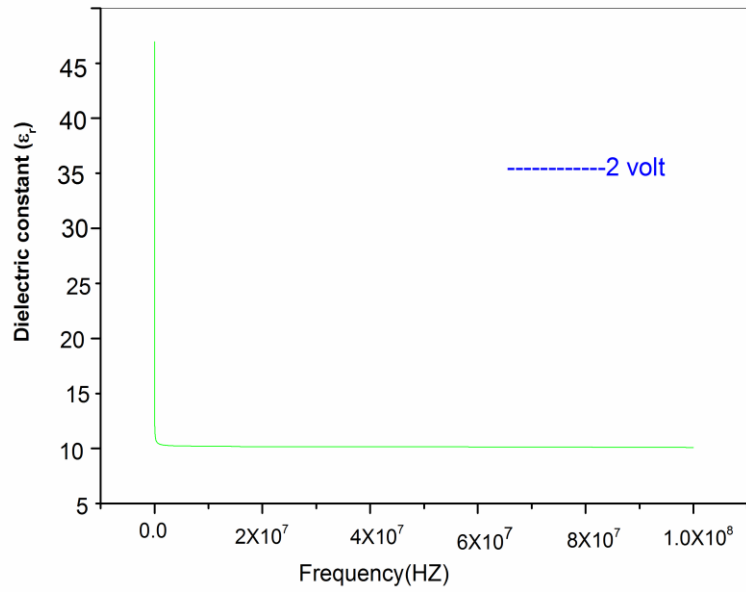
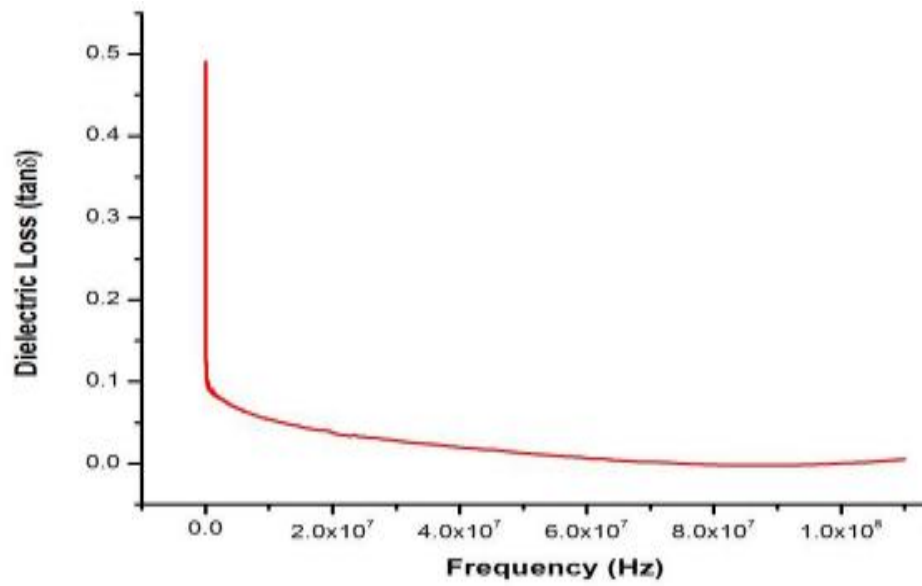
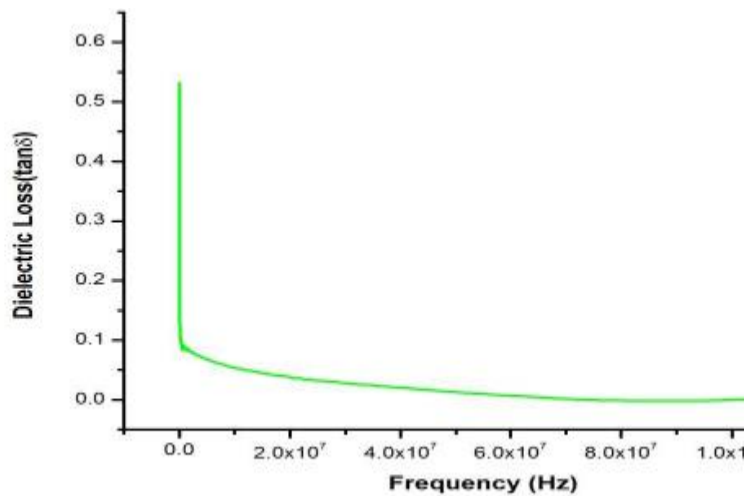


Figure 5.4.1 Dielectric constant ( $\epsilon_r$ ) vs. Frequency at different biasing voltage







**Figure 5.4.2 Dielectric Loss vs Frequency at different bias voltage for CCTO**

Dielectric constant ( $\epsilon_r$ ) and tangent loss ( $\tan\delta$ ) vs. frequency is for all the  $\text{CaCu}_3\text{Ti}_4\text{O}_{12}$  samples measured at  $900^\circ\text{C}$ . The samples were measured at room temperature with different external bias voltage from 0 to 4V and within a frequency range 1 kHz to 100kHz. Initially, the value of dielectric constant ( $\epsilon_r$ ) in all the samples is quite large, which is gradually decreased on increasing the frequency and finally reached a constant value at high frequencies. The variation of loss tangent ( $\tan\delta$ ) values with frequency also follows similar patterns at all biasing voltages (fig 5.4.1 & fig 5.4.2). Due to space charge polarization, this nature of graphs occurs within  $10^5$  Hz. This phenomenon is due to phase lag with applied external field. Phase lag occurs due to the inertia effect of the effective mass response with applied frequency. Above dielectric nature also indicates probable non-linear current-voltage characteristics following non-ohmic behavior. It may be due to probable Schottky-type electrostatic barrier formation at the grain boundaries.



## **CHAPTER-6**



## **CONCLUSION & FTURE SCOPE**

## Conclusion

Calcium Copper Titanate (CCTO) is successfully synthesized by modified solid state route. XRD result show the peaks corresponding to cubic perovskite structure. The disordering in sample decreases with increase in milling time if heat treated at same temperature. Moreover, XRD result show the formation of single phase with 30 milling and heat treated at 900<sup>0</sup>C. The FESEM image shows formation of well defined grain. The grain size increases with increasing milling activation time with high porosity. Dielectric studies of samples reveals that the dielectric constant is quite large, which is gradually decreased on increasing the frequency and finally attained a constant value at high frequency. The enhancement of dielectric properties is lead to device fabrication applications.

## Future Scope

The desired result can be obtained by optimizing process parameter .Moreover; the doping of Calcium Copper Titanate (CCTO) with transition metals might be beneficial to obtain better dielectric properties of the present system.

## REFERENCE



## References

- [1] IEC 60137:2003. 'Insulated bushings for alternating voltages above 1,000 V.' IEC,2003
- [2] Ramirez,A.P.,et al.,Giant dielectric constant response in a copper-titante Solide State Communications,2000. 115(5):p.217-220
- [3] Subramanian,M.A., et al., High Dielectric constant in  $ACu_3Ti_4O_{12}$  and  $ACu_3Ti_3FeO_{12}$  Phase. Journal of Solid State Chemistry, 2000.151(2):p.323-325
- [4] "Dielectrics-physics".Britannica.2009. P .1 Retrieved 2009-08-12
- [5] Electronics, optics, solid-state physics and cell biophysics
- [6] HyperPhysics-Electricity and magnetism.
- [7] Subramanian, M. A.; Li, Dong; Duan, N.; Reisner, B. A.; Sleight, A. W. (2000-0501). "High Dielectric Constant in  $ACu_3Ti_4O_{12}$  and  $ACu_3Ti_3FeO_{12}$  Phases". Journal of Solid State Chemistry. **151** (2): 323–325. doi:10.1006/jssc.2000.8703.
- [8] Ramirez A P,Subramanian M A, GardelM, Blumberg G, Li D,Vogt T and Shapiro S M 2000 Solid State Commun. **115** 217-20
- [9] Sinclair D C, Adams T B, Morrison F D and West A R 2002 Appl.Phys. Lett.802153
- [10] Ramirez A P,Subramanian M A, GardelM, Blumberg G, Li D,Vogt T and Shapiro S M 2000 Solid State Commun. **115** 217-20

- [11] K.Thomas Jacob , Chander Shekhar , Xiaogan Li, Girish M. Kale *Acta Shapiro S M* 2000  
*Solid State Commun.* 115217-20
- [12] Smith, A.E., et al., *An anion substitution route to low loss colossaldielectric CaCu<sub>3</sub>Ti<sub>4</sub>O<sub>12</sub>*.  
*Journal of Solid State Chemistry*,2009. **182**(2): p. 409-411.
- [13] Chung S, Kim I and Kang S 2004 **3** 774–8
- [14] Ramirez M A, Bueno P R, Varela J A and Longo E 2006 *Appl. Phys.Lett.*892121024798  
4803
- [15] Marques V P B, Bueno P R, Simoes A Z, Cilense M, Varela J A, Longo E and Leite E R  
2006 *Solid State Commun.*138
- [16] Ramirez A P, Lawes G, Li D and Subramanian M A 2004 *Solid State Commun.* **131**251–5
- [17] C. C. Homes, T. Vogt, S. M. Shapiro, S. Wakimoto, and A. P. Ramirez,*Science  
Appl.Phys.Lett.*131251-5
- [18] D. C. Sinclair, T. B. Adams, F. D. Morrison, and A. R. West D. C. Sinclair, T. B. Adams, F.  
D. Morrison, and A. R. West *Appl. Phys. Lett.* 80, 2153 (2002)
- [19] W. Si, E. M. Cruz, P. D. Johnson, P. W. Barnes, P. Woodward, and A. P. Ramirez *Appl.  
Phys. Lett* 81, 2056 (2002).
- [20] G. Deng, T. Yamada, and P. Muralt *Appl. Phys Lett.* 91202903 (2007).
- [21] G.Deng, N. Xanthopoulos and P. Muralt *Appl. Phys. Lett.* 92,172909 (2008)
- [22] C. C. Homes, T. Vogt, S. M. Shapiro, S. Wakimoto, and A. P. Ramirez, *Science Appl. Phys.  
Lett.* **293**, 673(2001).
- [23] C. C. Homes, T. Vogt, S. M. Shapiro, S. Wakimoto, and A. P. Ramirez, *Science Appl. Phys.  
Lett.* **293**, 673(2001).
- [24] D. C. Sinclair, T. B. Adams, F. D. Morrison, and A. R. West D. C. Sinclair, T. B. Adams, F.  
D. Morrison, and A. R. West *Appl. Phys. Lett.* 80, 2153 (2002)
- [25] W. Si, E. M. Cruz, P. D. Johnson, P. W. Barnes, P. Woodward, and A. P. Ramirez *Appl.  
Phys. Lett* 81, 2056 (2002).
- [26] C. C. Homes, T. Vogt, S. M. Shapiro, S. Wakimoto, and A. P. Ramirez, *Science Appl. Phys.  
Lett.* **293**, 673(2001).

[27] Ramirez, A.P., et al., Giant dielectric constant response in a copper-titanate Solid State Communications, 2000. 115(5):p.217-220

[28] F. Rossignol, A. Rumeaud, T. Lebey, E. Dutarde B. Barbier, C. Combettes, S. Guillemet Fritsch, T. Chartier, 2009, 29, 731-735.

[29] Preparation of CCTO Powder by Solid State reaction by Kshitij C Prasad

[30] Julie J. Mohamed, Sabar D. Hutagalung, M. Fadzil Ain, Karim Deraman, Zainal A. Ahmad, Materials Letters 61 (2007) 1835–1838

[31] Synthesis and characterization of  $\text{CaCu}_3\text{Ti}_4\text{O}_{12}$  and lanthanum doped by auto-combustion technique by Sunil patra.

[32] Synthesis and characterization of  $\text{CaCu}_3\text{Ti}_4\text{O}_{12}$  and lanthanum doped by auto-combustion technique by Sunil Patra .

[33] Ben Peng Zhua, ZiYu Wanga, Yue Zhanga, ZhiSong Yua, b, Jing Shia, c, Rui Xiong, Materials Chemistry and Physics, 2009, 113, 746-748.

[34] P. Thomas, K. Dwarakanath, K.B.R. Varma, T.R.N. Kutty, Journal of Physics and Chemistry of Solids, 2008, 69, 2594-2604.

[35] G. Chiodelli, V. Massarotti, D. Capsoni, M. Bini, C.B. Azzoni, M.C. Mozzatic, P. Lupotto, Solid State Communications, 2004, 132, 241-246.

[36] Alexander Tselev, Charles M. Brooks, Steven M. Anlage, Physical Review 70, 2004, 144181.

[37] K D MANDAL, ALOK KUMAR RAI, LAXMAN SINGH and OM PARKASH 2012

[38] Almeida AFL, de Oliveira RS, Goes JC, et al. *Mater Sci Eng B* 2002;96:275

[39] Sahaya Shajan X, Mahadevan C. *Cryst Res Technol* 2005;40:598.

[40] Sahaya Shajan X, Mahadevan C. *Cryst Res Technol* 2005;40:598.

[41] Thomas P, Dwarakanath K, Varma KBR, et al. *J Phys Chem Solids* 2008;69:2594.

## Appendix





## 1. Calculations

1) For starting powders



$$\begin{aligned}\text{Weight of CaCO}_3 &= 1 \times 40.08 + 1 \times 12.01 + 3 \times 16 \\ &= 100.09 \text{ g}\end{aligned}$$

$$\begin{aligned}\text{Weight of CuO} &= 1 \times 63.55 + 1 \times 16 \\ &= 79.55 \text{ g}\end{aligned}$$

$$\begin{aligned}\text{Weight of TiO}_2 &= 47.87 + 16 \times 2 \\ &= 79.88 \text{ g}\end{aligned}$$

$$\begin{aligned}\text{Weight of CaCu}_3\text{Ti}_4\text{O}_{12} &= 1 \times \text{CaCO}_3 + 3 \times \text{CuO} + 4 \times \text{TiO}_2 = 100.09 + \\ &238.65 + 319.60 = 614.27 \text{ g}\end{aligned}$$

For 1 mol of CCTO 1 mol of  $\text{CaCO}_3$ , 3 mol of  $\text{CuO}$  and 4 mol of  $\text{TiO}_2$  required.

→ For 614.27 g of CCTO, 658.27 g of mixture was required

→ For 200 g of CCTO, 214.2 g of mixture was required

Weight of  $\text{CaCO}_3$  required = 32.4 g

Weight of  $\text{CuO}$  required = 77.6 g

Weight of  $\text{TiO}_2$  required = 104.0 g

2) For PVA calculation

3% PVA solution is there

2% PVA is to be added.

→ Weight of PVA = 0.6192

100 ml of PVA solution → 3 gram

3 gram → 100 ml

1 gram → 100/3ml

0.6192 gram → 2 .06 ml

→ Volume of PVA to added =2 ml

## 2. Formulae

- (1) Scherrers formula for particle size (t) determine from XRD analyses:

$$t = 0.9\lambda/\beta\cos\theta$$

wher, t is the particle size of the sample

$\lambda$  is the x-ray wavelength

$\beta$  is the linear boardining at half of the maximum intensity in radians

$\theta$  is the Bragg angle in degree

- (2) Determination of dielectric constant ( $\epsilon_r$ ):

$$\epsilon_r = (Cs d)/ A \epsilon_0$$

$\epsilon_r$  is the dielectric constant of the sample

d is the thickness of pellet

A is the area of the metalised portion of one surface of the pellets.



## **Phase Formation and Morphological Features of Calcium Copper Titanate by Modified Solid State Process**

**ASHNARAYAN SAH,<sup>1</sup> SOUMYA MUKHERJEE,<sup>2\*</sup>  
MOHAMMED SHAHNAWAZ<sup>3</sup> and SATH BANERJEE<sup>1</sup>**

<sup>1</sup>Department of Metallurgical and Materials Engineering, Jadavpur University,  
Kolkata - 700032, West Bengal, India.

<sup>2</sup>Department of Metallurgical and Materials Engineering, Kazi Nazrul University,  
Asansol - 713340, West Bengal, India.

<sup>3</sup>Department of Electronics and Telecommunication Engineering, Heritage Institute of Technology,  
Kolkata - 700107, West Bengal, India.

### **Abstract**

Perovskite calcium copper titanate possesses giant dielectric constant making it suitable candidate for possible applications in microelectronic components, advanced transistors, energy storage capacitors. Generally, this grade of material is synthesized by chemical route to improve homogeneity, controlled size growth for enhanced properties. In the present research, simple synthesis process was adopted using precursors of high purity oxides like Calcium carbonate, titania, Copper oxide without any use of complicated synthesis routes and costly chemical precursors. Molar ratio of oxides used was about 1:3:4 with mechano-chemical activation in agate mortar for 20, 25 and 30 hours respectively in dry condition. After milling, powders obtained were made to undergo annealing at fixed temperature of 900 °C for 26 hours soaking period. Phase analysis was carried to determine the phase along with crystallite size calculation. Bonding information of the synthesized sample was analyzed to obtain the M-O coordination and vibration - stretching analysis of the bonds. Morphological features were also noted using FESEM (Field Emission Scanning Electron Microscopy) for understanding grains and granular boundaries. Both FTIR (Fourier Transform Infra Red Spectroscopy) and XRD (X - Ray Diffractogram) analyses confirm the compound formation in terms of molecular structure responsible to obtain the proper phase.



### **Article History**

Received: 07 March 2019

Accepted: 12 April 2019

### **Keywords:**

Calcium Copper  
FTIR;  
Morphology;  
Titanate;  
XRD.

**CONTACT** Soumya Mukherjee ✉ [smmukherjee3@gmail.com](mailto:smmukherjee3@gmail.com) 📍 Department of Metallurgical and Materials Engineering, Kazi Nazrul University, Asansol - 713340, West Bengal, India.



© 2019 The Author(s). Published by Oriental Scientific Publishing Company

This is an Open Access article licensed under a Creative Commons Attribution-NonCommercial-ShareAlike 4.0 International License  
Doi: <http://dx.doi.org/10.13005/msri/160105>

## Introduction

Perovskite having  $ABO_3$  formula is a versatile ceramic structure with applications as semiconductor, catalyst, sensors, memory devices and others. Calcium Copper titanate is a modified perovskite structure material (also referred as aurivillius structure) having applications in the above mentioned domain in addition to application as magnetic materials after doping. The parent structure of perovskite is modified due to superimposition of body centered ordering of Ca, Cu along with prominent tilting of Titanium centred octahedral.<sup>1</sup> The ceramic is also known as colossal relative permeability due to high dielectric constant of about  $10^4$ . High dielectric constant also influences the volume of the electrical devices in applications. The origin for large dielectric constant is still under investigations. It has been reported in research studies that  $TiO_2$  and perovskite oxide lose oxygen during high temperature sintering while reoxidation occurs during cooling. During cooling re-oxidation occurs at the surface layers and at the grain boundaries as a cause of rapidly falling temperature and availability of short time. As a consequence, insulating layers are formed at surface and grain boundaries while the bulk grain remains semiconducting in nature.<sup>2</sup> The giant dielectric constant of the material is found to be almost independent of temperature in the range 100 - 400K. Chung *et al.* observed non-linear dielectric coefficient in the ceramic perovskite to be about 900 quite higher than ZnO which is used as classical varistor. Calcium copper titanate also exhibits high dielectric loss limiting its application in the domain of devices. This hindrance of the material is made to overcome by undergoing substitution at proper site. The scientific reason behind such suppression of dielectric loss may be due to retardation of barrier layer formation at grain boundaries. Material is noted to follow non-ohmic characteristics at such conditions.<sup>3</sup> The mentioned perovskite is observed to be synthesized by sol-gel process<sup>1,4,5,6</sup> mechanochemical process<sup>7,8</sup> solid state processing<sup>9,10</sup> hydrothermal<sup>11</sup> and others. Some other popular methods of synthesis are combustion synthesis method or self propagating high temperature synthesis, sonochemical assisted and co-precipitation technique. Calcium copper titanate is noted to be applied for capacitors, antennas, microwave devices and sensors. Porous polycrystalline nanostructure is found to be quite

beneficial for sensor applications. One of the significant properties of Calcium Copper titanate based sensor is the ability to detect, monitor gases and toxic species without decomposition or changes in their molecular arrangement.<sup>12</sup> In the present article, modified solid state process is adopted to synthesize utilizing proper molar ratio. The synthesized material is analyzed for phase determination by XRD, stretching bonding and M - O co-ordinations by FTIR analysis while morphology is studied by FESEM.

## Experimental Procedure

In the synthesis of perovskite (Aurivillius) Calcium Copper Titanate, Calcium Carbonate, Cupric Oxide and titania (AR Grade, Merck India) were selected as precursors. All the powders were taken in a proper stoichiometric ratio of  $CaCO_3:CuO:TiO_2$  as 1:3:4 and made to undergo milling activation in arid condition. Milling activation was carried for 20 hours, 25 hours and 30 hours respectively followed by annealing at 900 °C for 26 hours. Phase analysis was carried by XRD (Rigaku, Ultima III,  $Cu K\alpha 1.54\text{\AA}$ , 50KV, 40mA) for synthesized powder samples. Scan range for the sample was 10 to 90° with scan rate of 5°/min along with determination of crystallite size and planes of orientation. Morphology of the sample was studied using FESEM, Hitachi S-4800 in powder state. The sample was placed on carbon tape with conducting coating over it to prevent static charge accumulation for better resolution and imaging. Bonding and metal co-ordination analysis was carried for powder samples by FTIR analysis (IR Prestige - 21, Shimadzu) after mixing it with KBr for pellet preparation. Pellets were prepared for FTIR analysis by undergoing pressing under pressure of 6t /  $cm^2$  in hydraulic press.

## Results and Discussions

Above figures execute XRD of the synthesized samples. In all cases sharp intense peaks are noted without any convolution or peak splitting. Intense sharp peaks are indications of crystalline nature of the synthesized materials. There is no trace of diffuse peaks or humps in the material matrix. The XRD patterns confirm the single phase structure. All three samples are made to undergo three different milling time variations but same soaking period at constant temperature of about 900 °C is maintained. At this fixed composition sharp peaks are noted

within the  $2\theta$  scan range at  $34.55^\circ$ ,  $38.8^\circ$ ,  $49.50^\circ$  and  $61.65^\circ$  respectively. Small peaks can also be observed about  $2\theta$  values of  $27.75^\circ$ ,  $35.80^\circ$ ,  $42.60^\circ$  and  $75.30^\circ$  respectively. The peaks are indexed as per the (hkl) planes reported in JCPDS file (75 - 1149). Appearance of peaks corresponding to CCTO phase indicates formation of single phase compound. The above XRD peaks are in correspondence with findings by N. Tripathy *et al.*,<sup>13</sup> R. E. - González *et al.*<sup>7</sup> where synthesis is carried by solid state routes followed by sputtering and mechanochemical process. Some minor impurities like copper oxide is noted at about  $35.88^\circ$  after 20 hours milling, 26 hours annealing at  $900^\circ\text{C}$ . Similarly for 25 hours milling minor peaks of impure oxides of Ti is noted respectively. For 30 hours milling, sample is noted to be the most pure without any formation of other metal oxides instead of desired perovskite

compound. Crystallite size obtained by Scherrers formula is noted to be about 84.47 nm, 82.66 nm for 20 hrs, 30 hours sample and around 122 nm for 25 hours mill sample. The sudden change may be due to formation of TiO as noted from XRD analysis. TiO is metastable in nature formed as intermediate during milling which later converts to perovskite after milling reaction followed by annealing. Due to development of minor secondary phase, nucleation, growth of phases undergo metastabilization and hence such possible drastic increase in crystallite size happens. Moreover, 30 hours milling followed by 26 hours heat treatment leads to pure calcium copper titanate without any presence of other oxides as noted from XRD analysis with reference to JCPDS of Titanium oxide (81 - 1286), Copper Oxide (80 - 1917) used as precursors.

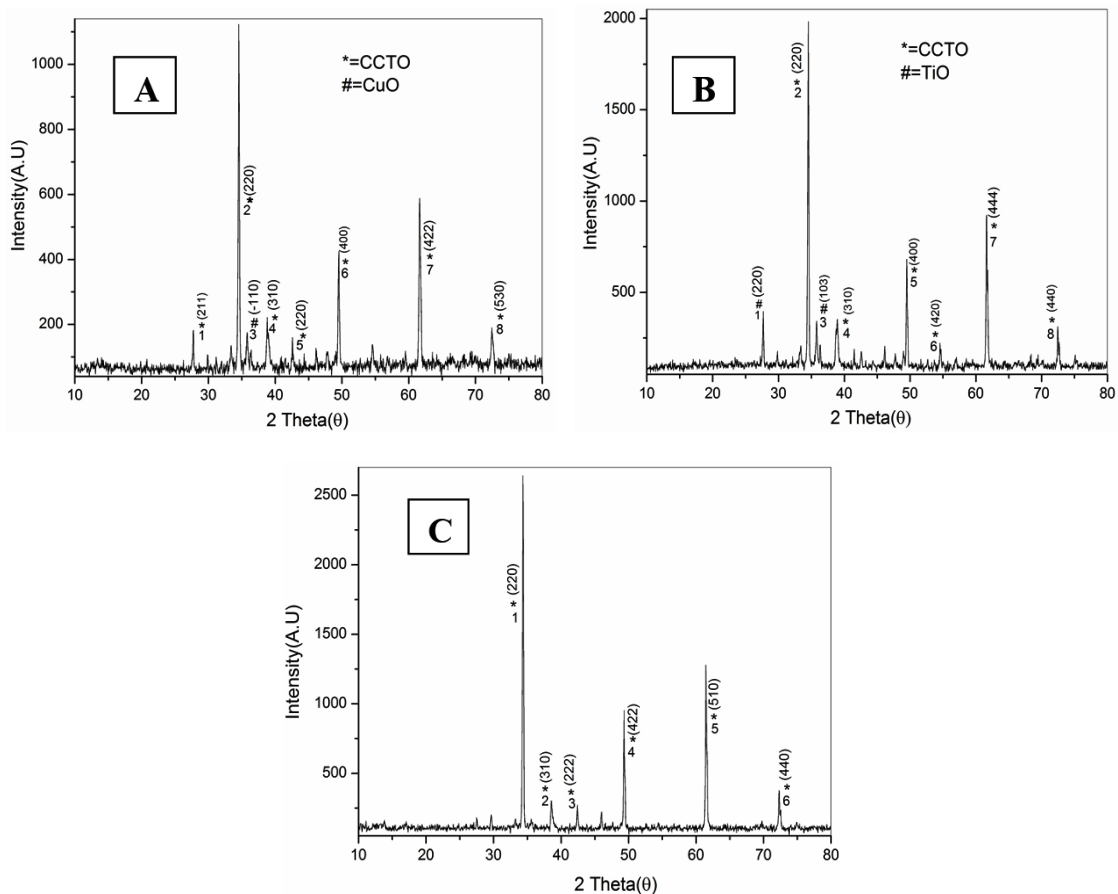


**Fig. 1: XRD of Calcium Copper Titanate synthesized after 20hrs milling (A), 25hrs milling (B) and 30 hours milling (C) activation after soaking at  $900^\circ\text{C}$  for 26 hours**

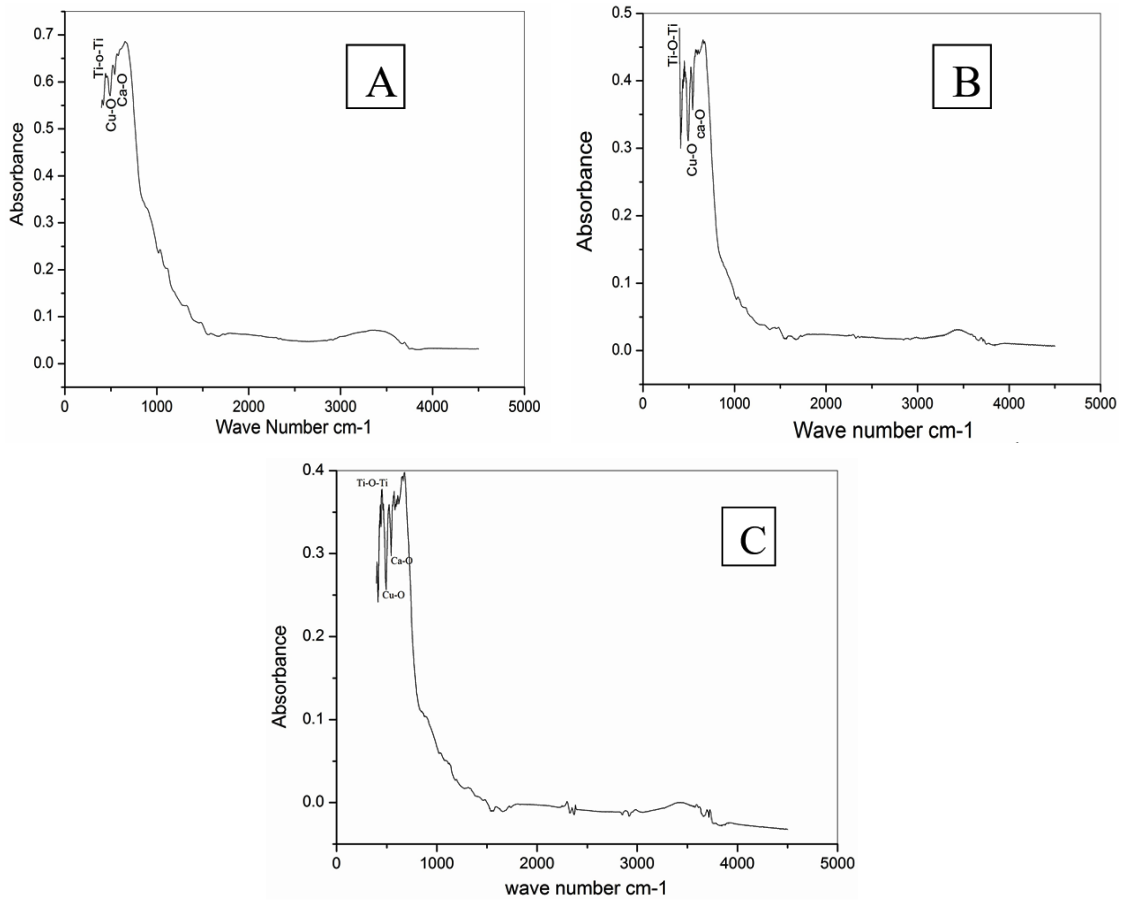


**Fig. 2: FTIR of Calcium Copper Titanate synthesized after 20hrs milling (A), 25hrs milling (B) and 30 hours milling (C) activation after soaking at 900°C for 26 hours**

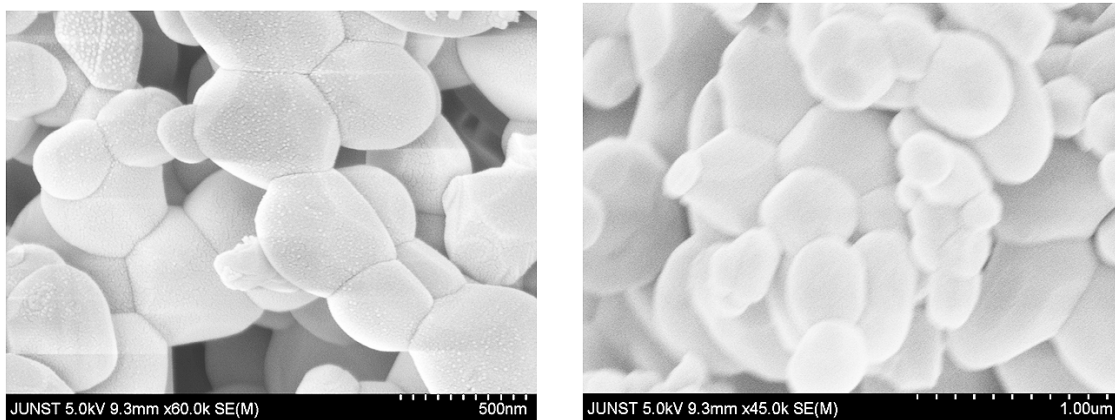


**Fig. 3: FESEM morphology of Calcium Copper Titanate formed after 30 hours milling activation after soaking at 900°C for 26 hours**

Figure 2 represents FTIR spectra of the synthesized samples. Major peaks of vibration for M-O coordinations are noted within  $1000\text{ cm}^{-1}$  indicating the successful synthesis of inorganic structure. Absorption peaks are noted at about  $530\text{ cm}^{-1}$ ,  $450\text{ cm}^{-1}$ ,  $500\text{ cm}^{-1}$  mainly. The above absorptions are corresponding to Ca-O, vibration mode of the O-Ti and bending of Cu-O bonds present in the synthesized samples. The experimental characteristics bands are noted within the scan range of  $380\text{ cm}^{-1}$  to  $700\text{ cm}^{-1}$  encompassing the mixture of  $\text{CuO}_4$  and  $\text{TiO}_6$  groups. The above experimental bands and peaks indicate presence of CCTO as sample validating the XRD phase determination. The above experimental findings are in correspondence with the results of P. Thirumanathan *et al* who have studied optical, electrical properties of sol-gel synthesized calcium copper titanate powders.<sup>5</sup> Almeida observed three main absorptions at  $561$ ,  $516$ ,  $437\text{ cm}^{-1}$  and Ti-O vibrations at about  $653\text{-}550\text{ cm}^{-1}$  while for Ti-O-Ti it is about  $495\text{-}436\text{ cm}^{-1}$ .<sup>14</sup> Thus above findings are noted to be in correspondence with research article by Almeida *et.al* which focussed on mechanochemical alloying of Calcium copper titanate.

FESEM morphology of the best synthesized conditioned sample is noted after confirming the s from phase analysis and FTIR analysis on bonding, M-O information. From XRD analysis it is concluded that 30 hours milling followed by 26 hours soaking period at  $900\text{ }^\circ\text{C}$  yields the most pure perovskite. Morphology of the synthesized sample at the above mentioned conditions exhibit proper granular formation with strong agglomeration tendency. Few minute pores are noted within the agglomerated

form. Strong interconnections among grains are noted. Grains are having polygonal shape with conchoidal fracture face at top while some are having spherical morphology. Individual grains are around  $500\text{nm}$  to about  $200\text{nm}$ ,  $100\text{nm}$  in some cases. Grains are found to get interlocked in a particular fashion leading to floral one with conchoidal fracture granules around the central hub of the agglomerates. There is absence of any unwanted distortion observed in the matrix of the synthesized sample.

### Conclusions

Modified Solid State Process was utilized to prepare modified perovskite structure material Calcium Copper titanate. Crystallite size was noted to be about  $84.47\text{nm}$ ,  $82.66\text{nm}$  for 20 hrs, 30 hours sample and around  $122\text{ nm}$  for 25 hours mill sample. Bonding and stretching vibration analysis of M-O coordination were noted from FTIR analysis. FESEM analysis reveals the morphology to be granular in nature with strong agglomeration, minute porosity while grains were polygonal shape with conchoidal fracture.

### Acknowledgement

Corresponding would like to thank HOD, Department of Metallurgical & Materials Engineering for providing XRD facilities to study phase formation. Author also acknowledges Prof (Dr.) Kalyan Kumar Chappopadhyay, Director, SMSNT, Jadavpur Univerasity for providing FTIR and FESEM facilities.

### Funding Sources

There is no funding sources for carrying the experiment in the laboratory.

### References

1. Jesurani S., Kanagesan S., Velmurugan R., Kalaivani T. Phase formation and high dielectric constant of calcium copper titanate using sol-gel route. *J. Mater. Sc. Electron.* 2012;23:668-674.
2. Rai A. K., Singh N. K., Lee S. K., Mandal K. D., Kumar D., Om Parkash. Dielectric properties of iron doped calcium copper titanate,  $\text{CaCu}_2\text{9Fe0.1Ti}_4\text{O}_{12}$ . *J. Alloy. Compd.* 2011; 509:8901-8906.
3. Chung S. Y., Kim Il. D., Kang S. J. L. Strong nonlinear current-voltage behaviour in perovskite derivative calcium copper titanate. *Nat. Mater.* 2004;3:774-778.
4. Xu D., He K., Chen B., Xu Ch., Mua Sh., Lei. Jiao, Xi. Sun, Yang Y. Microstructure and electric characteristics of  $\text{AETiO}_3$  (AE=Mg, Ca, Sr) doped  $\text{CaCu}_3\text{Ti}_4\text{O}_{12}$  thin films prepared by the sol-gel method. *PRO. NAT. SCI-MATER.* 2015;25L:399-404.
5. Thiruramanathan P., Marikani A., Madhavan D. Optical and Electrical Properties of Sol-



- Gel Synthesized Calcium Copper Titanate Nanopowders. *Int. J. Chem. Tech. Res.* 2015;8 No. 3:981-987.
6. Jesurani S., Kanagesan S., Velmurugan R., Thirupathi C., Sivakumar M., Kalaivani T. Nanoparticles of the giant dielectric material, Calcium Copper titanate from a Sol-gel technique. *Mater. Lett.* 2011;65:3305-3308.
  7. González R. E., Vega E., Tamayo R., Criado J. M. Díaz M. J. Mechanical Processing of  $\text{CaCu}_3\text{Ti}_4\text{O}_{12}$  with Giant Dielectric Properties. *Mater. Manuf. Processes.* 2014;29:1179-1183.
  8. Alizadeha M., Ardakani H. A., Amini R., Ghazanfari M. R., Ghaffari M. Structural and phase evolution in mechanically alloyed calcium copper titanate dielectrics. *Ceram. Int.* 2013;39:3307-3312.
  9. A.P. Ramirez, M.A. Subramanian, M. Gardel, G. Blumberg, D. Li, T. Vogt, S.M. Shapiro, Giant dielectric constant response in a copper-titanate. *Solid. State. Commun.* 2000;115: 217–220.
  10. Yu, Tim & Liu, Hanxing & Hao, Hua & Guo, Liling & Jin, Chengjun & Yu, Zhiyong & Cao, Minghe. (2007). Grain Size Dependence of Relaxor Behavior in  $\text{CaCu}_3\text{Ti}_4\text{O}_{12}$  Ceramics. *Applied Physics Letters.* 91. 222911-222911. 10.1063/1.2820446.11.
  11. Oliveira L. H., de Moura A. P., Mazzo T. M., Ramírez M. A., Cavalcante L. S., Antonio S. G., Avansi W., Mastelaro V. R., Longo E., Varela J. A. Structural refinement and photoluminescence properties of irregular cube-like  $(\text{Ca}_{1-x}\text{Cu}_x)\text{TiO}_3$  microcrystals synthesized by the microwave hydrothermal method. *Mater. Chem. Phys.* 2012;136:130-139.
  12. Ahmadipour M., Ain M. F., Ahmad Z. A. A Short Review on Copper Calcium Titanate (CCTO) Electroceramic: Synthesis, Dielectric Properties, Film Deposition and Sensing Application. *Nano-Micro Lett.* 2016;8:291-311.
  13. Tripathy N., Das K. C., Ghosh S. P., Bose G., Kar J. P. Fabrication of high-k dielectric Calcium Copper Titanate (CCTO) target by solid state route. *IOP Conf. Series: Materials Science and Engineering.* 115 (2016) 012022 doi:10.1088/1757-899X/115/1/012022
  14. Almeida A. F. L., De Oliveira R. S., Go'és J. C., Sasaki J. M., Souza Filho A. G., Mendes Filho J., Sombra A.S.B. Structural properties of  $\text{CaCu}_3\text{Ti}_4\text{O}_{12}$  obtained by mechanical alloying. *Mater. Sci. and Engg. B.* 2002;96: 275-283.